Observational Evidence for Primordial Black Holes

Florian Kühnel
Max Planck Institute for Physics

New Horizons in Primordial Black Hole Physics
Naples, Italy — 19th of July 2023

Observational Evidence for Primordial Black Holes:

A Positivist Perspective

Florian Kühnel

Max Planck Institute for Physics

New Horizons in Primordial Black Hole Physics

Naples, Italy — 19th of July 2023

… usually:

Focus on Constraints

PBH Constraints

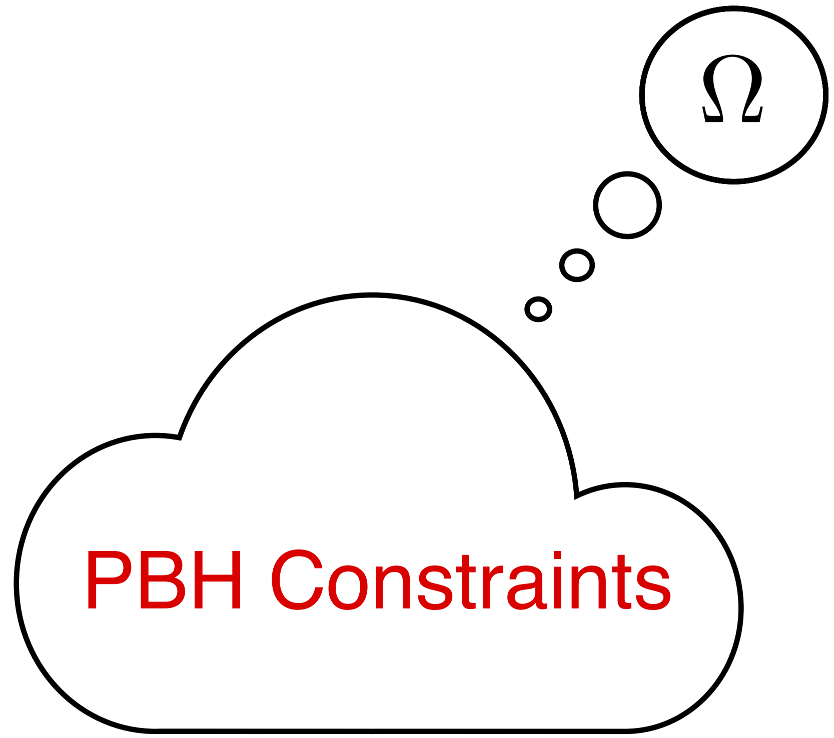
PBH Constraints
Ω

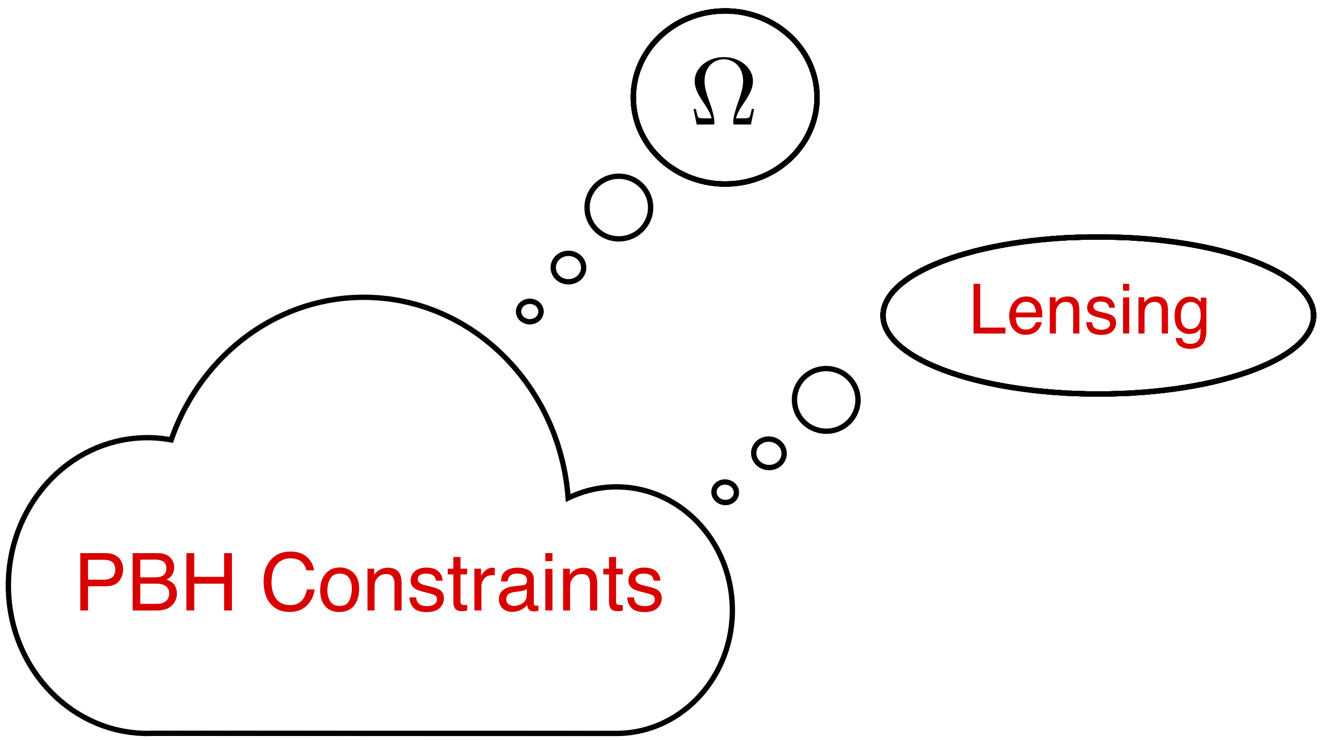

Ω
Lensing
PBH Constraints

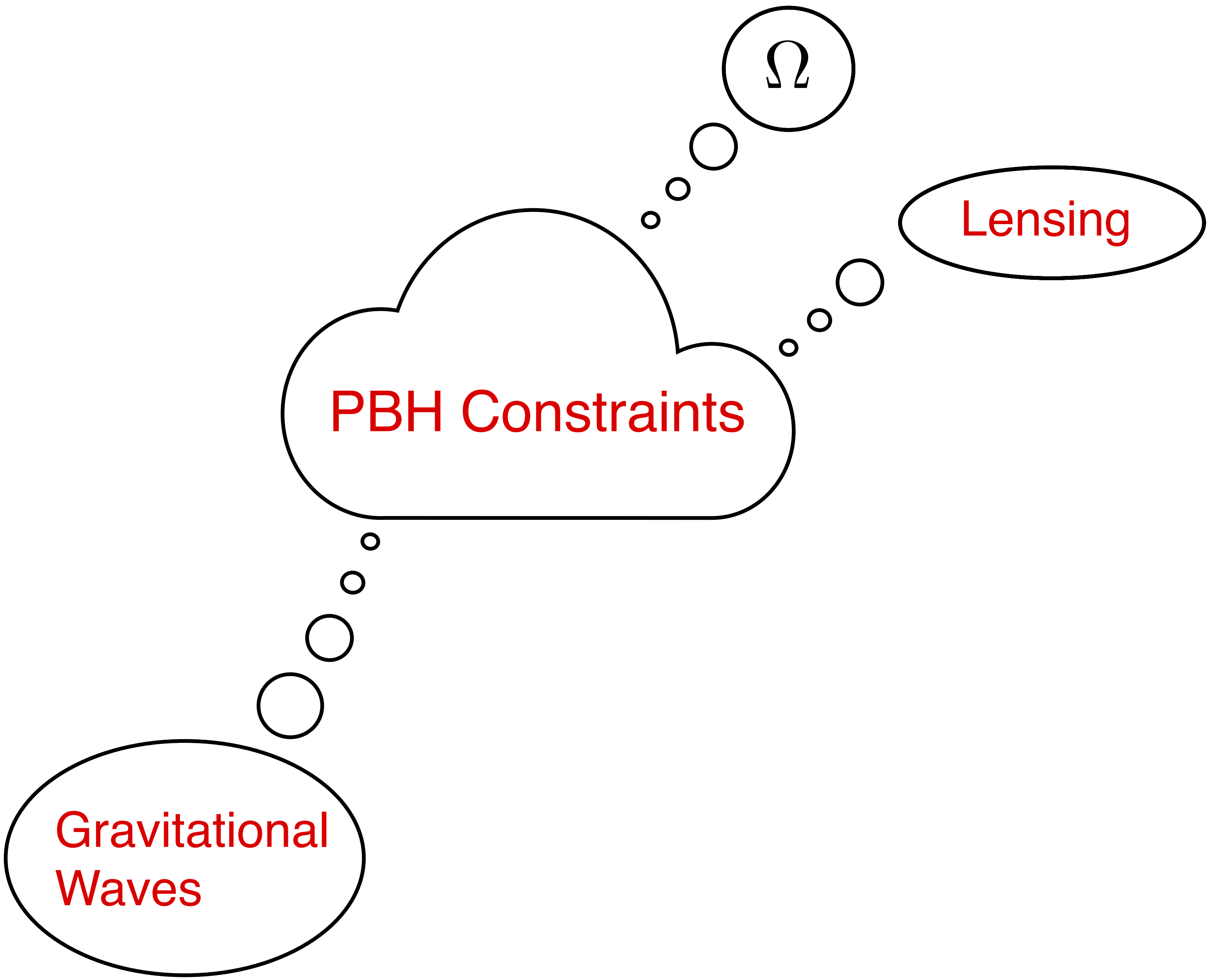
Ω
Lensing
PBH Constraints
Gravitational
Waves

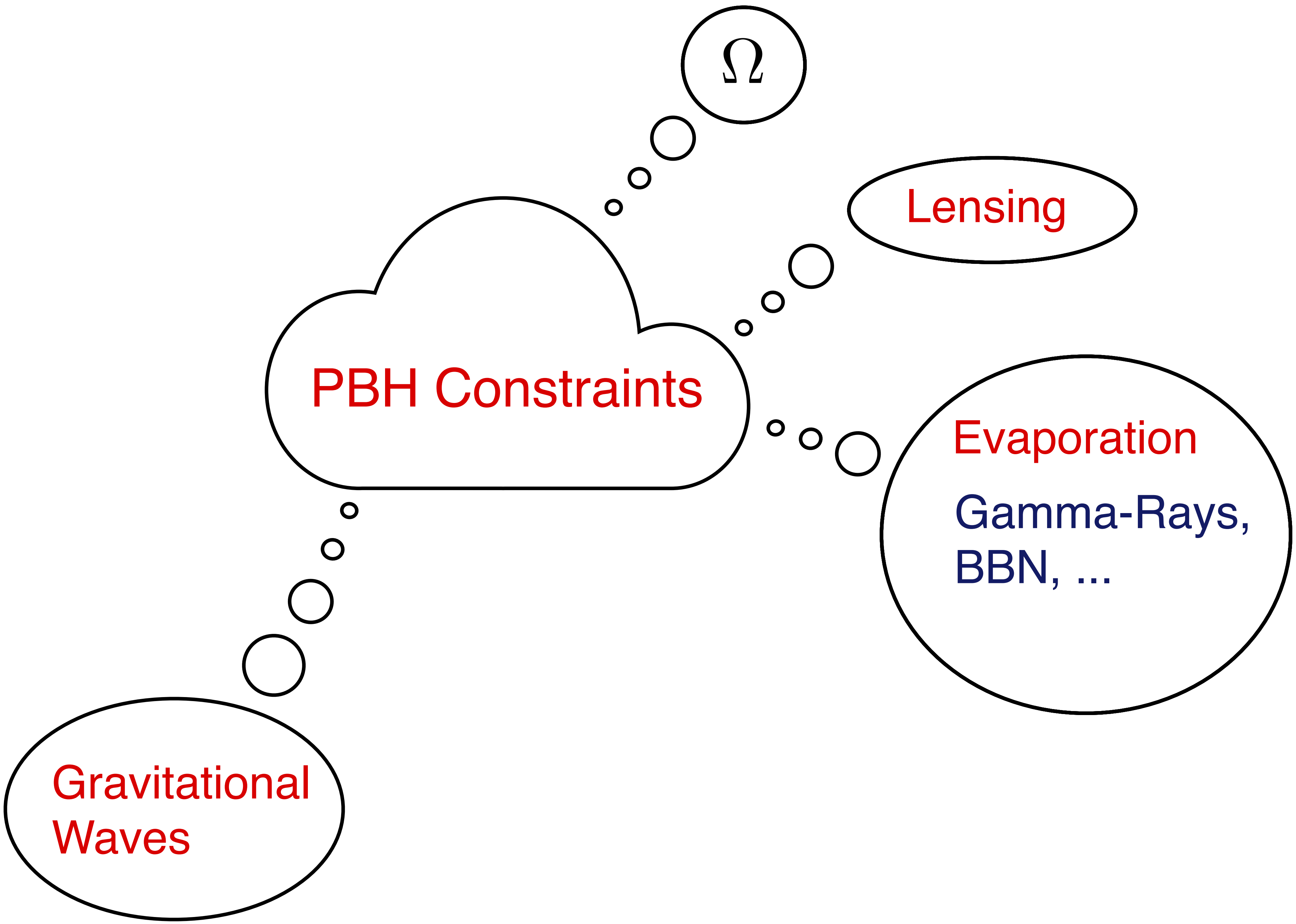
PBH Constraints
Ω
Lensing
Evaporation
Gamma-Rays,
BBN, ...
Gravitational
Waves

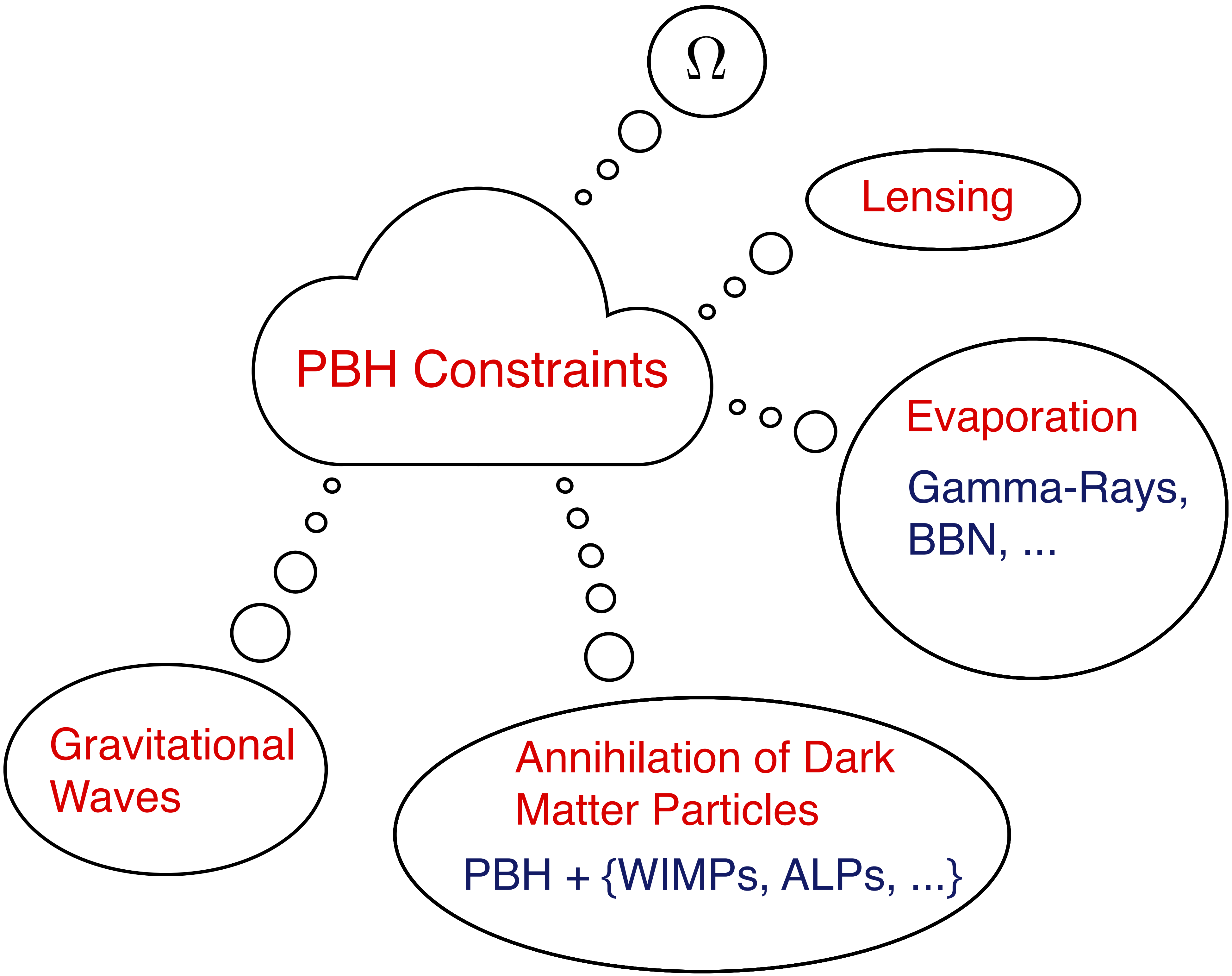
PBH Constraints
Ω
Lensing
Evaporation
Gamma-Rays,
BBN, ...
Gravitational
Waves
Annihilation of Dark
Matter Particles
PBH + {WIMPs, ALPs, ...}

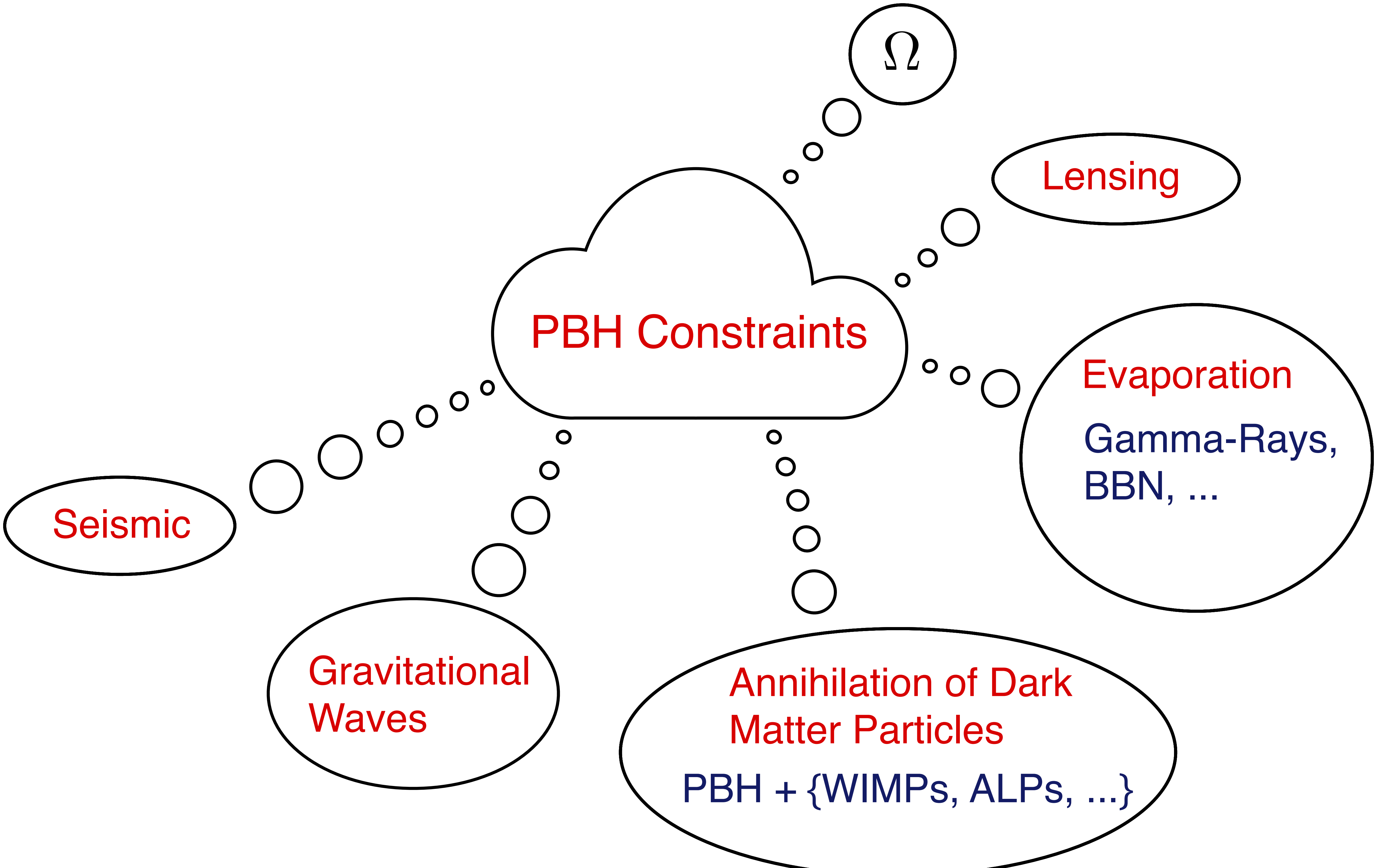

PBH Constraints
Ω
Lensing
Evaporation
Gamma-Rays,
BBN, ...
Seismic
Gravitational
Waves
Annihilation of Dark
Matter Particles
PBH + {WIMPs, ALPs, ...}

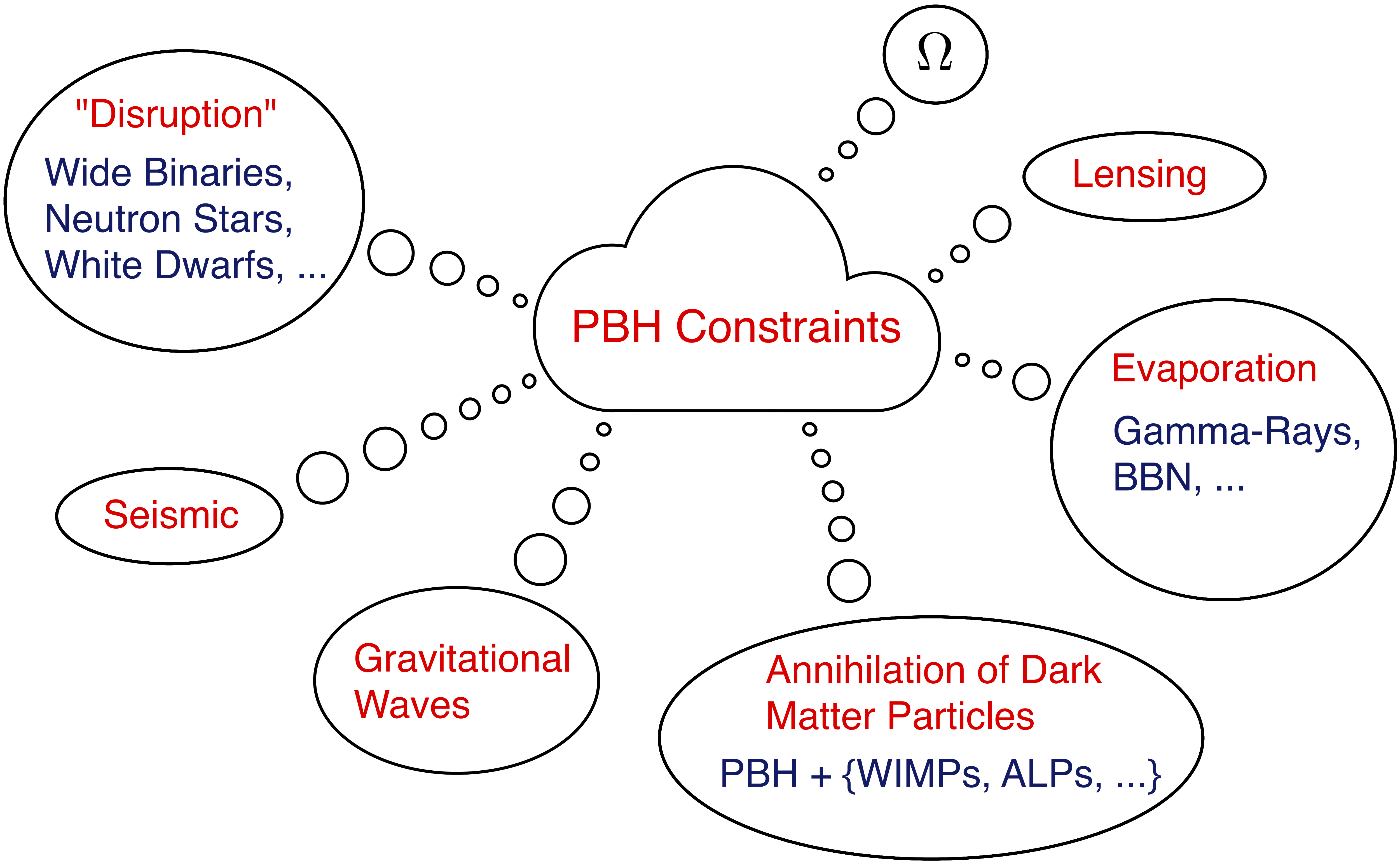
Ω
"Disruption"
Wide Binaries,
Neutron Stars,
White Dwarfs, ...
Lensing
PBH Constraints
Evaporation
Gamma-Rays,
BBN, ...
Seismic
Gravitational
Waves
Annihilation of Dark
Matter Particles
PBH + {WIMPs, ALPs, ...}

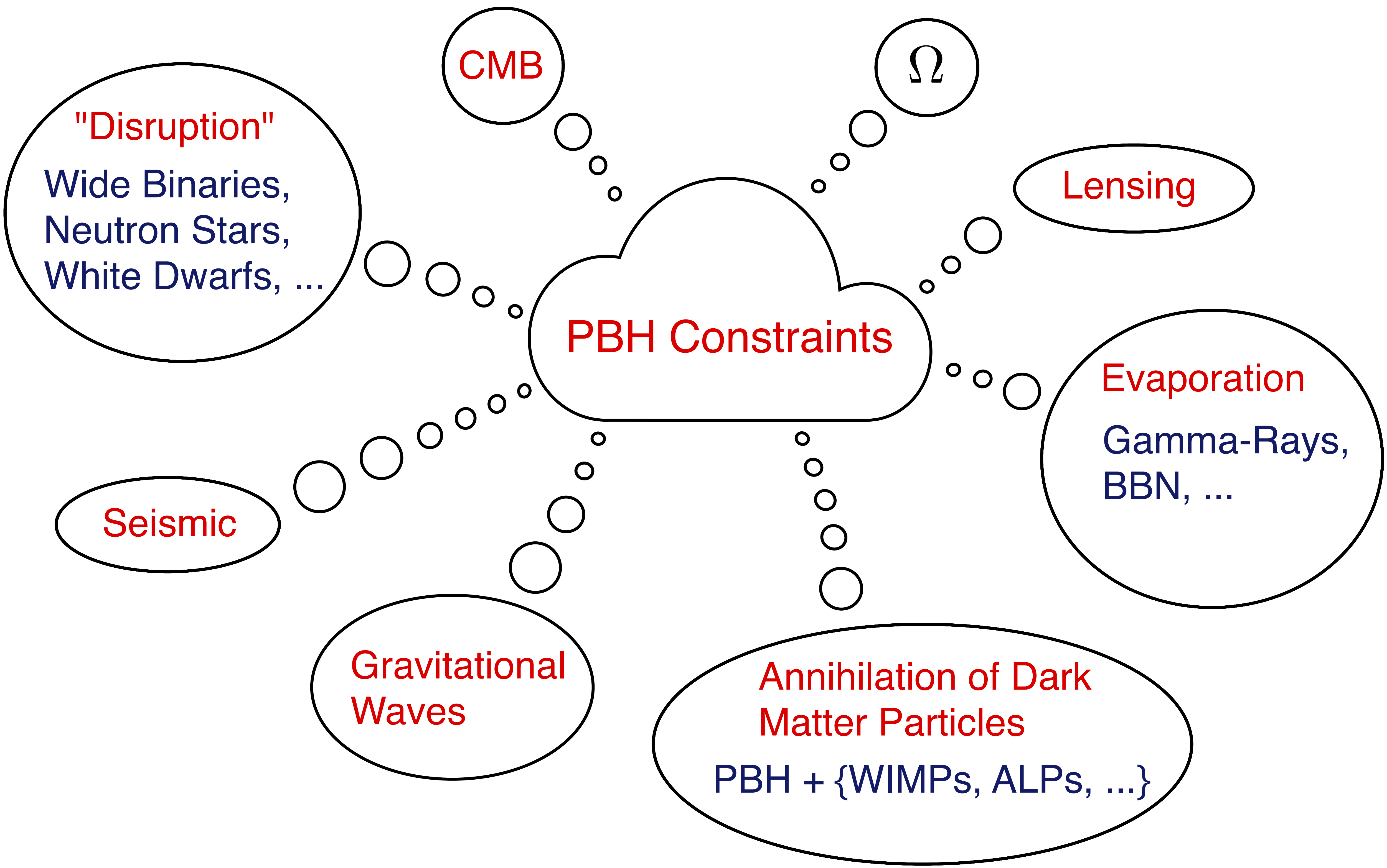
PBH Constraints
CMB
Ω
Lensing
"Disruption"
Wide Binaries,
Neutron Stars,
White Dwarfs, ...
Evaporation
Gamma-Rays,
BBN, ...
Seismic
Gravitational
Waves
Annihilation of Dark
Matter Particles
PBH + {WIMPs, ALPs, ...}

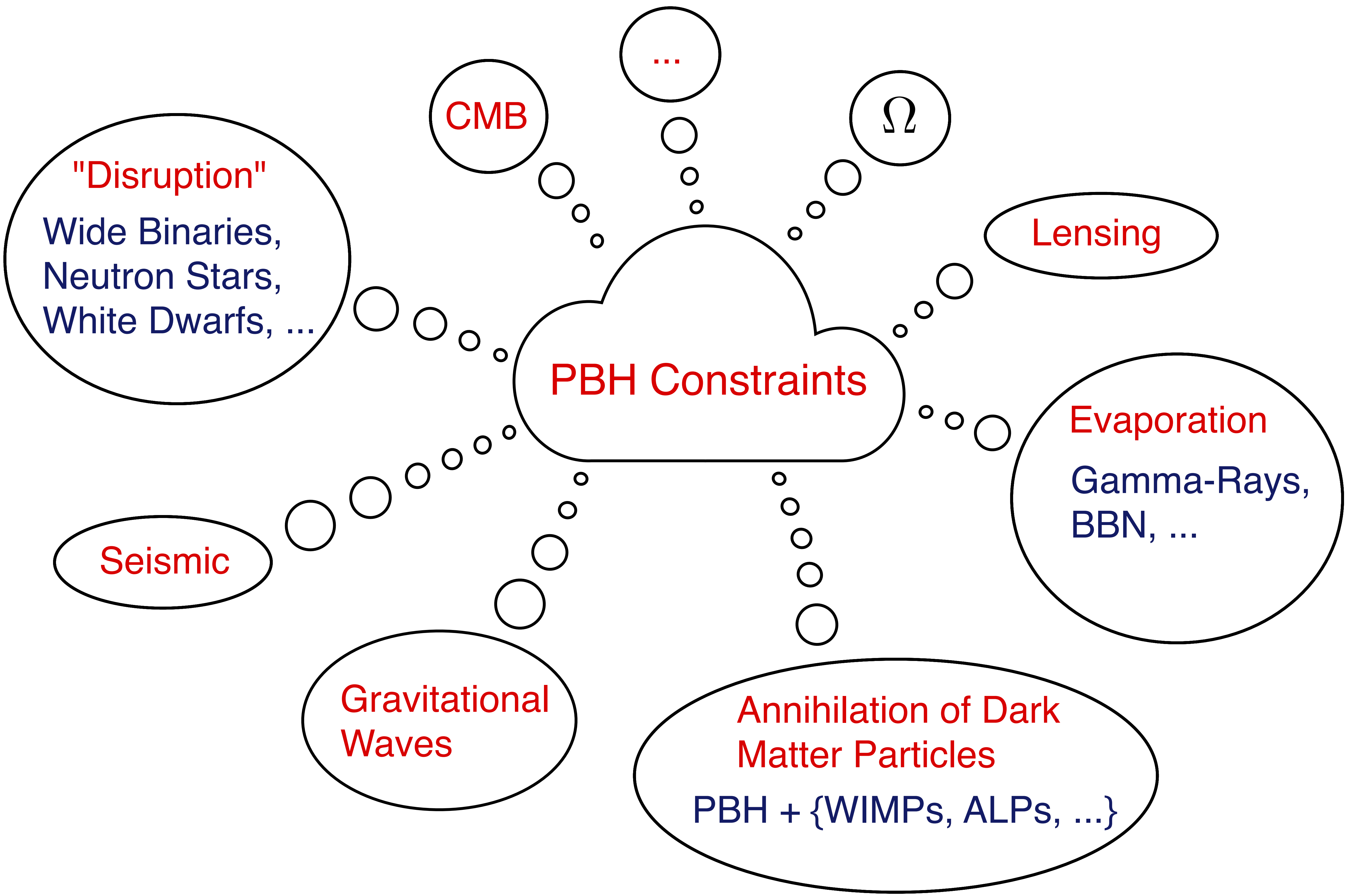
PBH Constraints
...
CMB
Ω
"Disruption"
Wide Binaries,
Neutron Stars,
White Dwarfs, ...
Lensing
Evaporation
Gamma-Rays,
BBN, ...
Seismic
Gravitational
Waves
Annihilation of Dark
Matter Particles
PBH + {WIMPs, ALPs, ...}

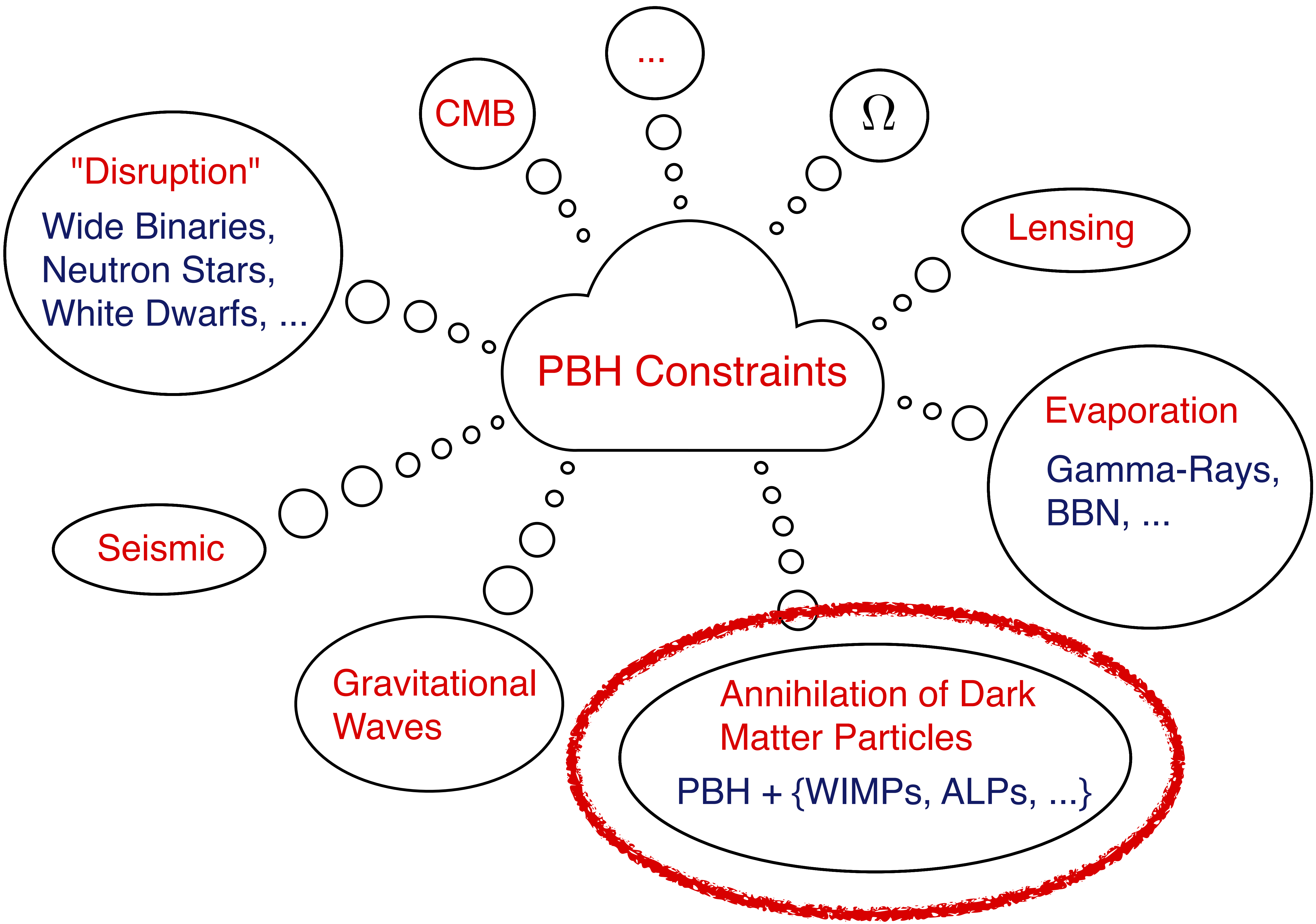
PBH Constraints
"Disruption"
Wide Binaries,
Neutron Stars,
White Dwarfs, ...
CMB
...
Ω
Lensing
Evaporation
Gamma-Rays,
BBN, ...
Seismic
Gravitational
Waves
Annihilation of Dark
Matter Particles
PBH + {WIMPs, ALPs, ...}

PBHs & WIMPs

Halo Profile

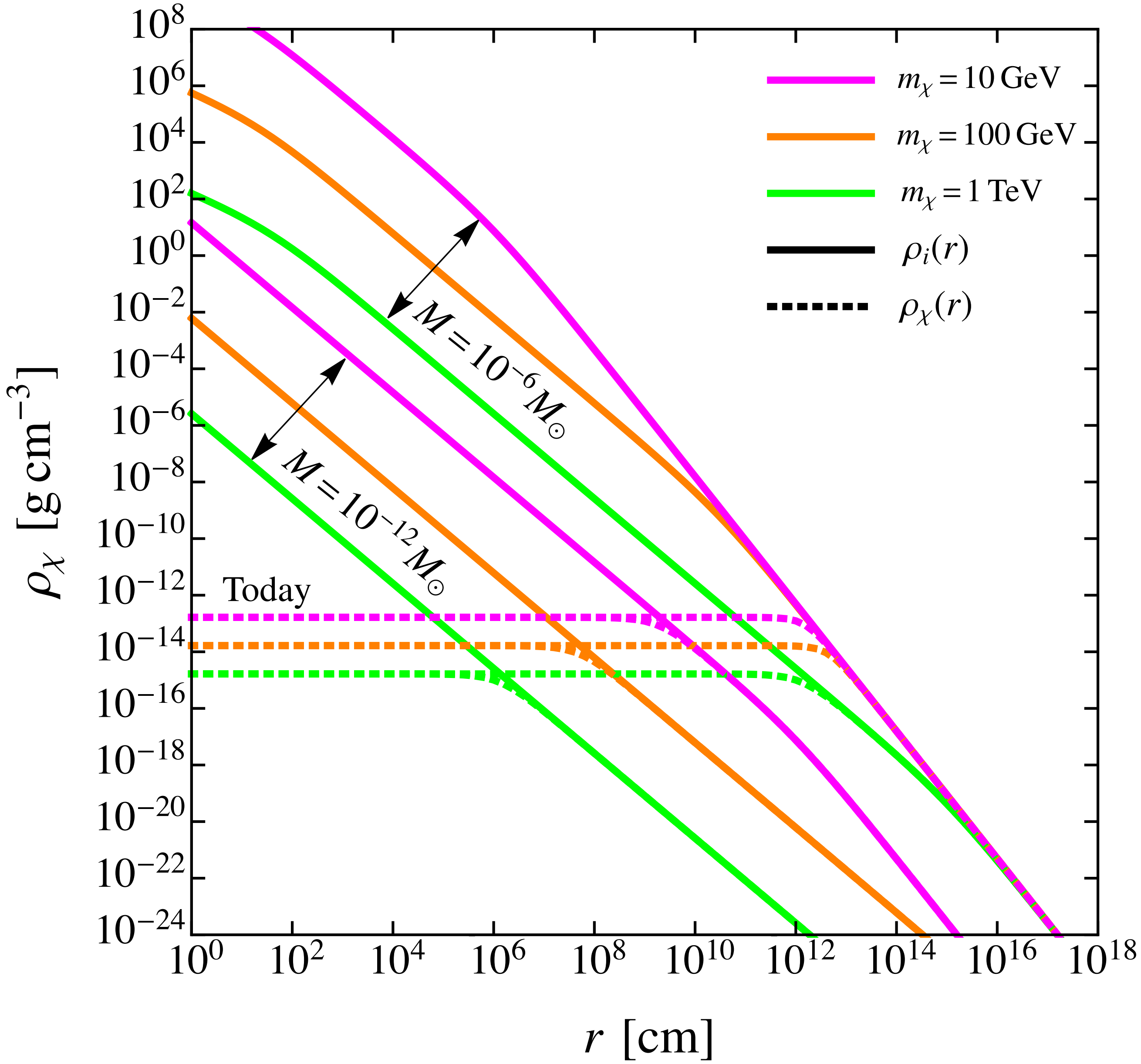

[Carr, FK, Visinelli 2021]

PBHs & WIMPs

Halo Profile

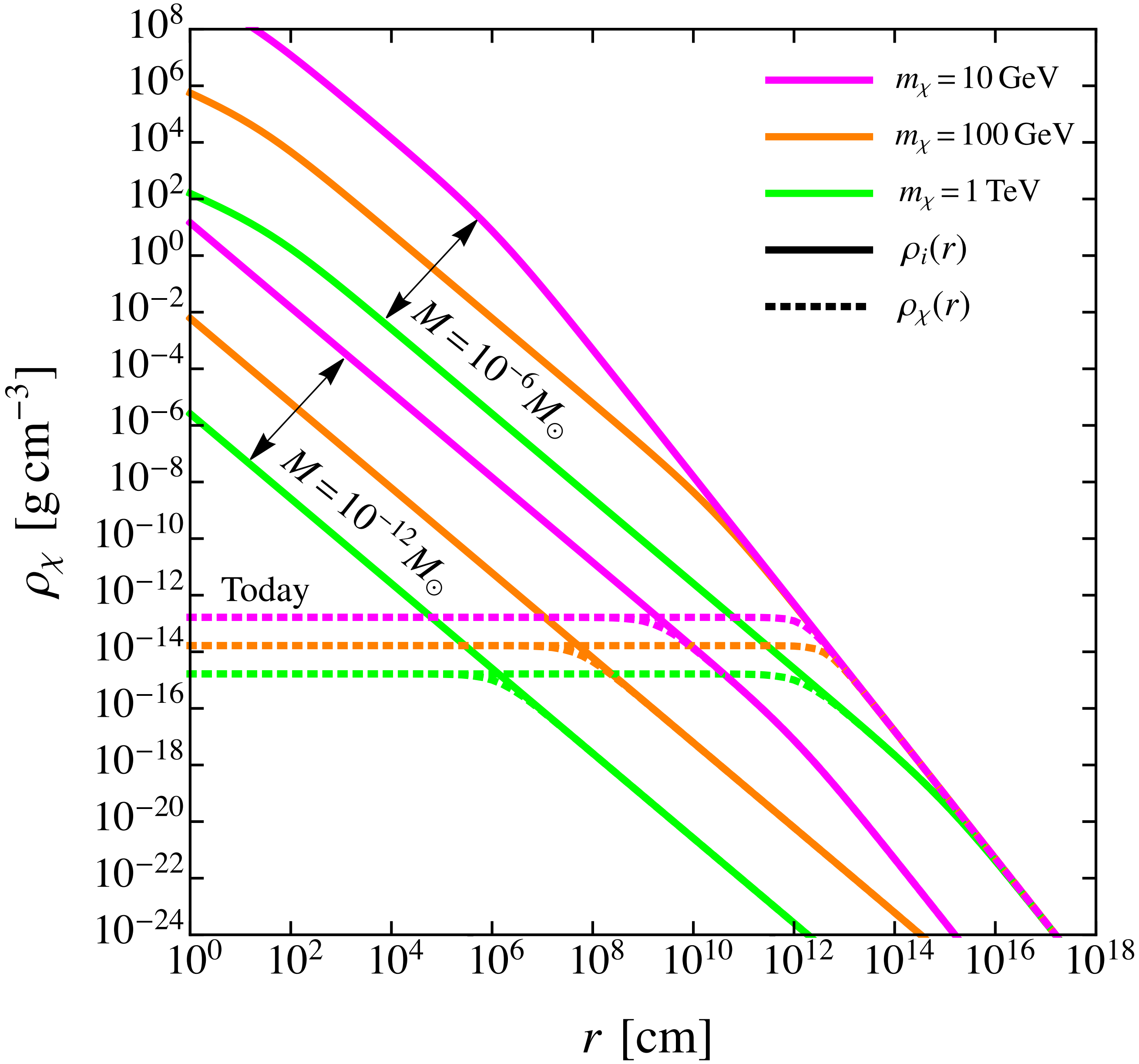

PBH Constraints

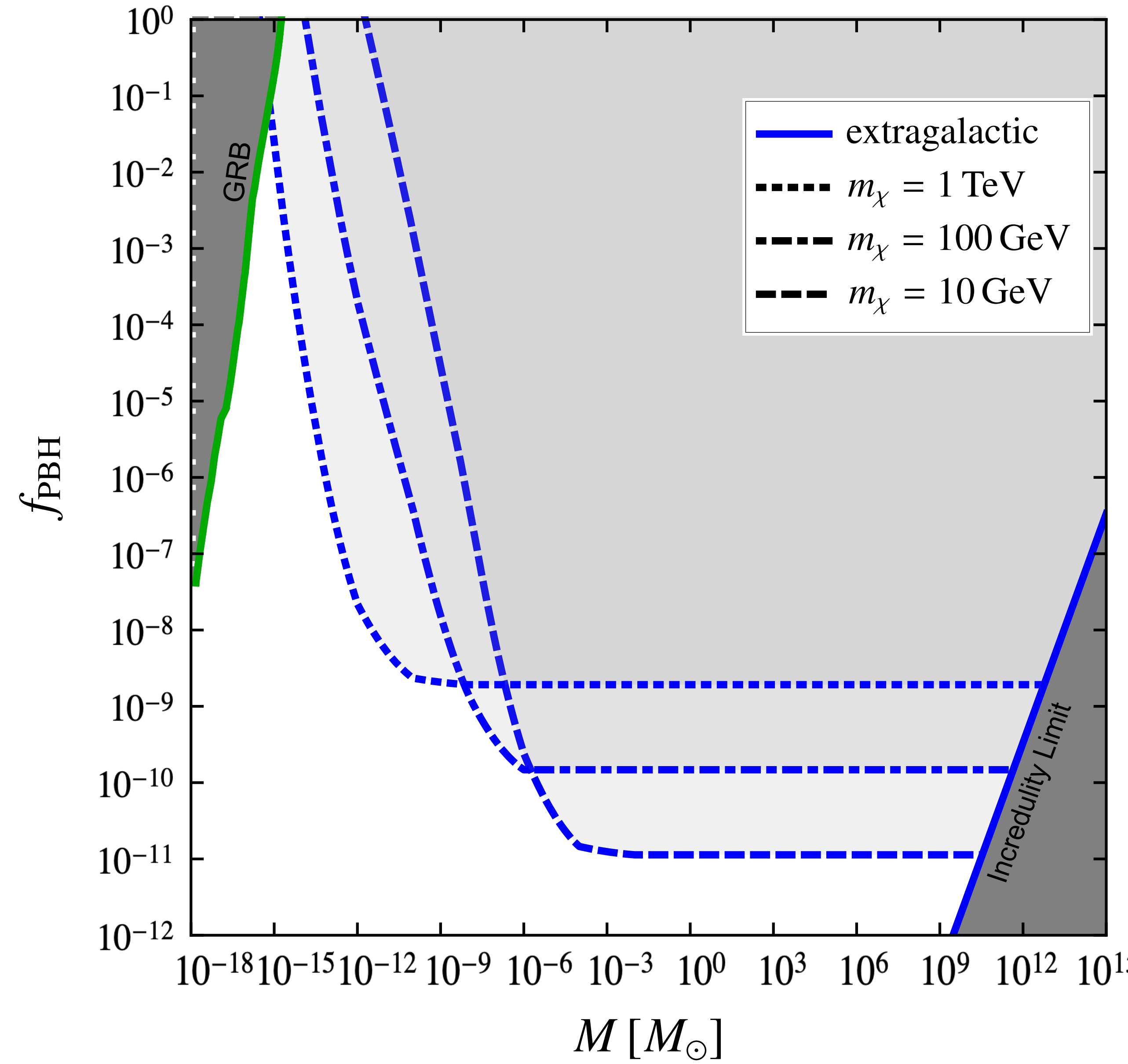

[Carr, FK, Visinelli 2021]

PBHs & WIMPs

Halo Profile

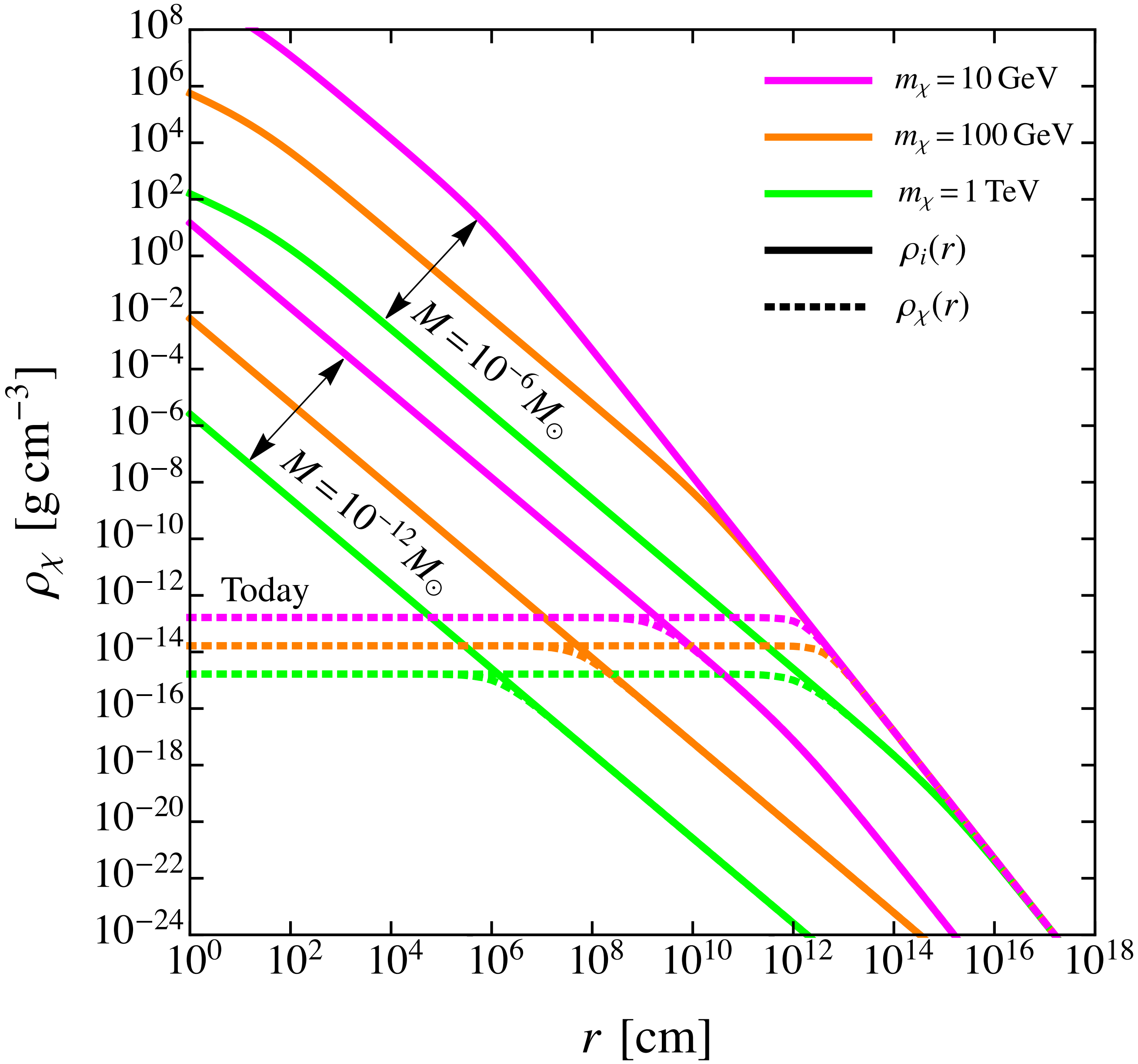

PBH Constraints

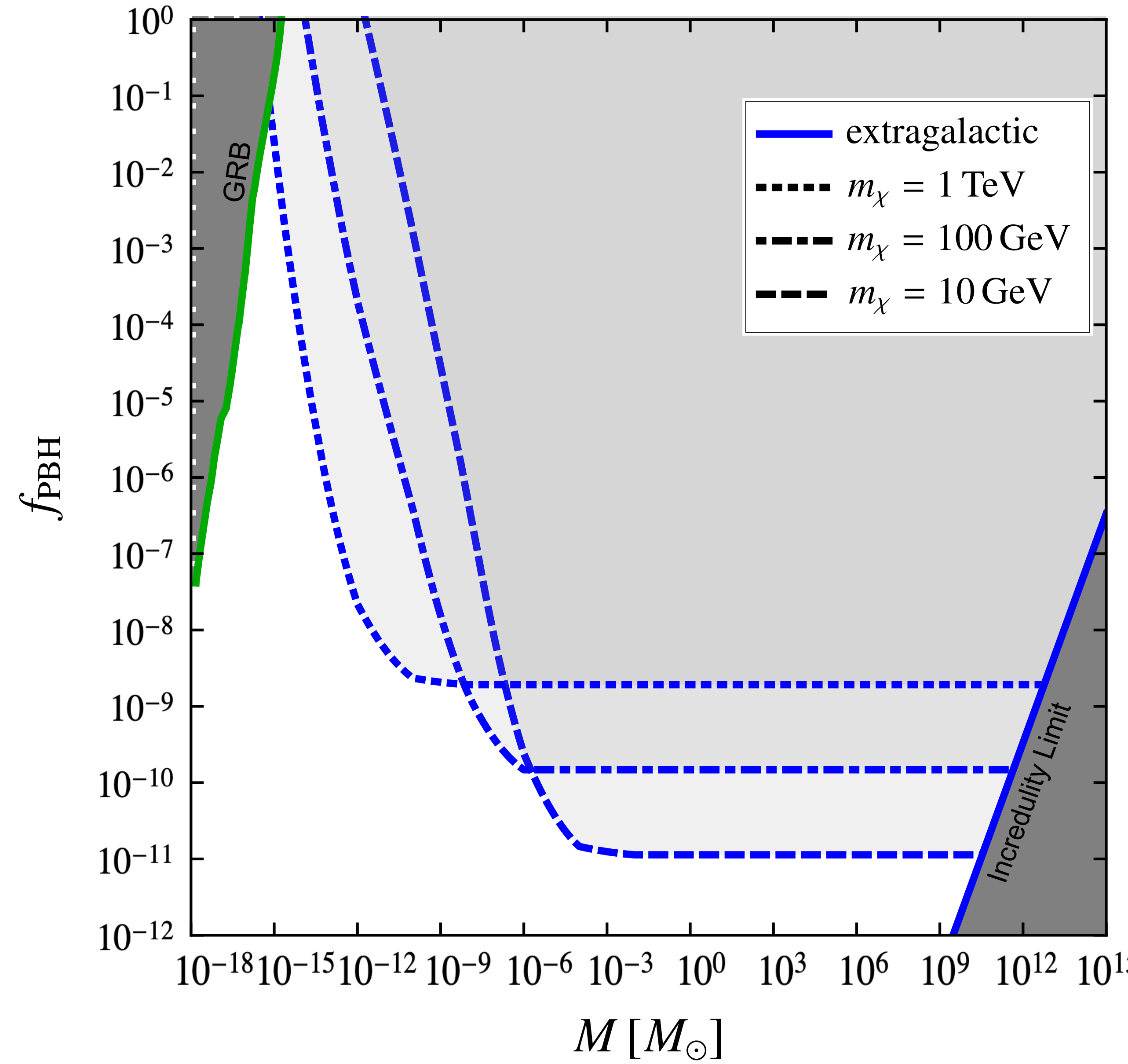

[Carr, FK, Visinelli 2021]

★ PBHs (on a large mass range) and (standard) WIMPs are incompatible!

A Positivist Perspective:

Observational Hints for Primordial Black Holes

A Positivist Perspective:

Evidence

Observational ~~Hints~~

for Primordial Black Holes

Planetary-Mass Microlensing

★ OGLE detected a particular population of microlensing events:

★ 0.1 - 0.3 days light-curve timescale - origin unknown!
Could be free-floating planets... or PBHs!

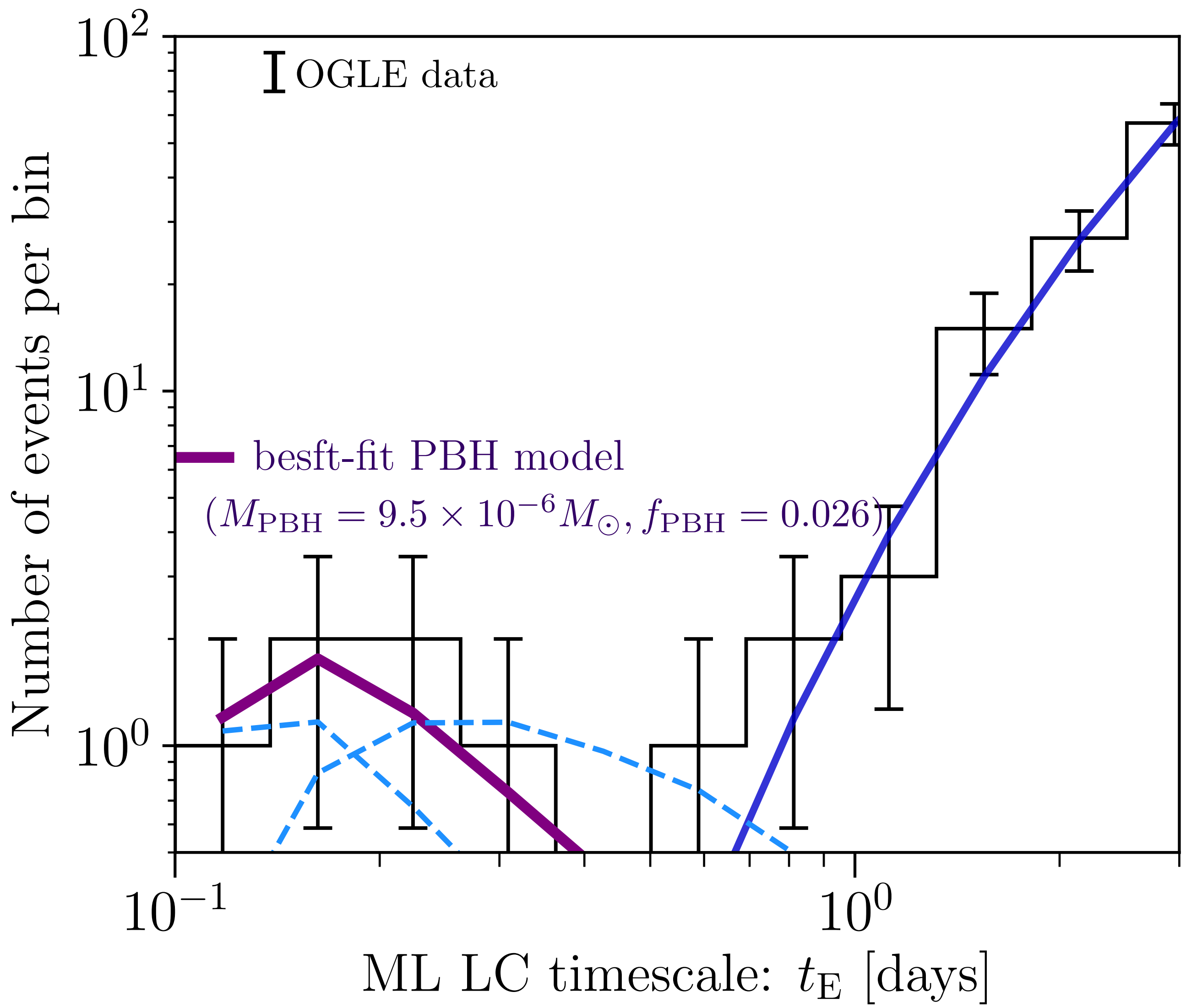

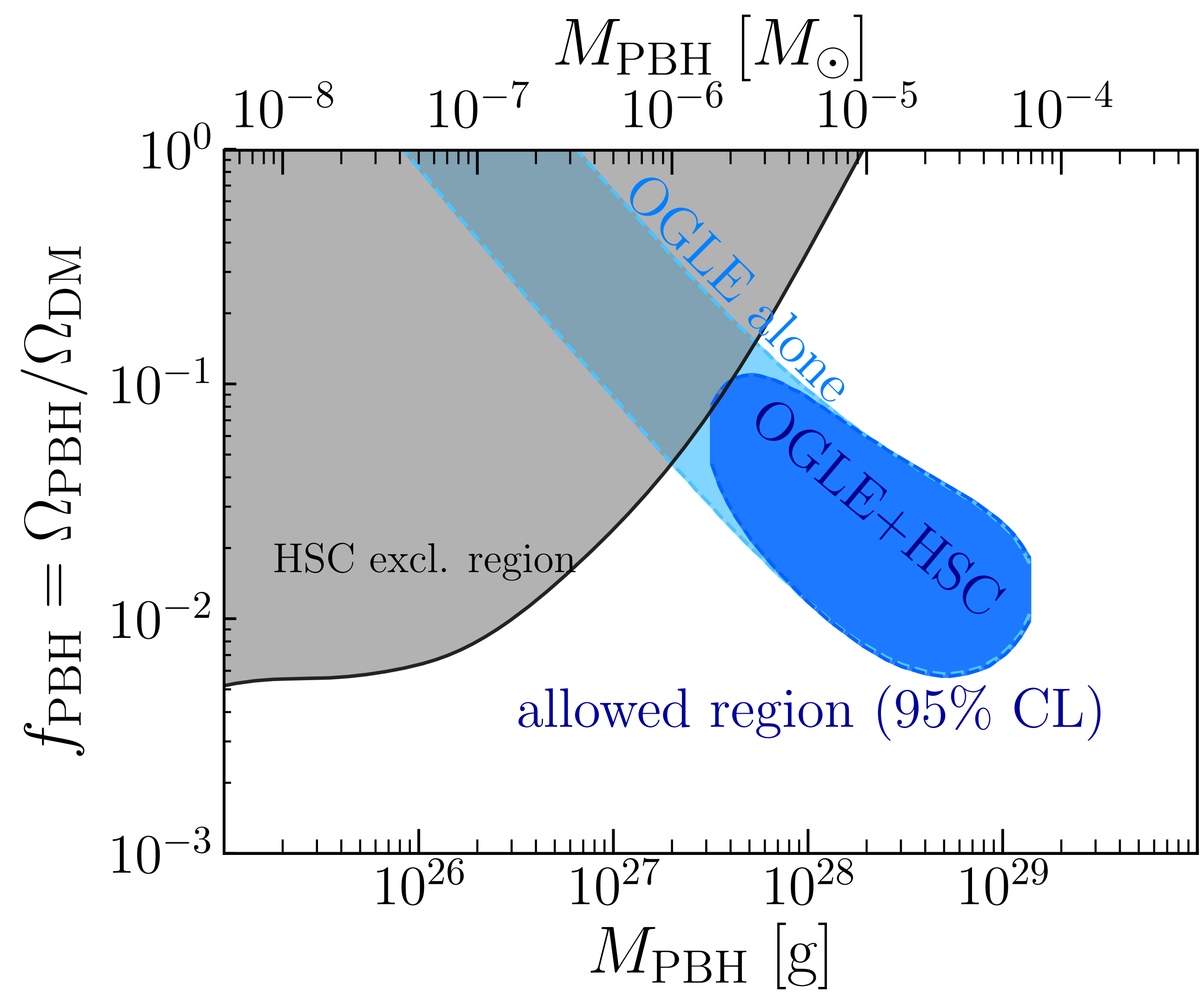

[Niikura *et al.* 2019]

Excess of Lenses in Galactic Bulge

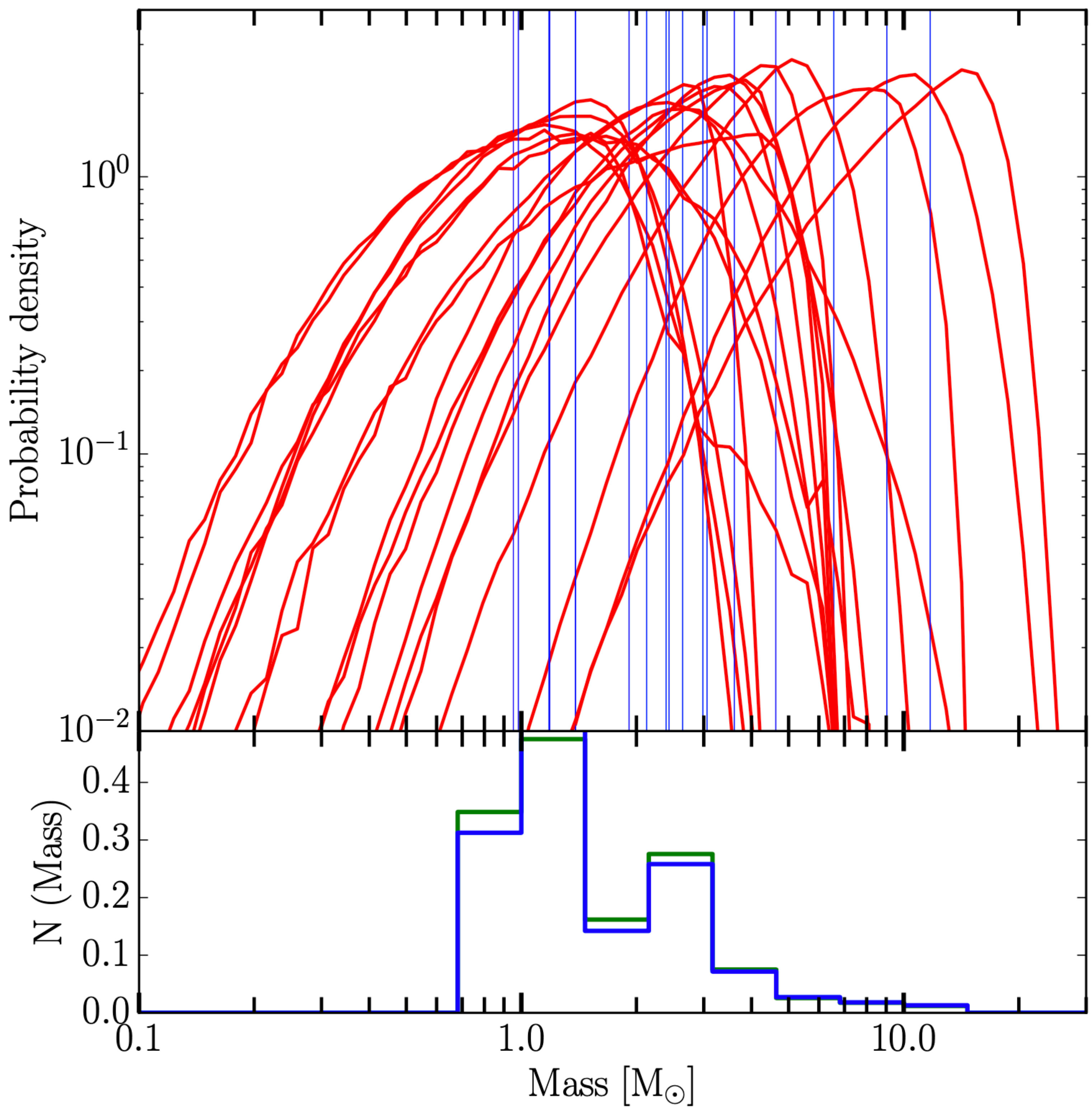

- OGLE has detected 58 long-duration microlensing events in the Galactic bulge.
- 18 of these cannot be main-sequence stars and are very likely black holes.
- Their mass function overlaps the low mass gap from 2 to 5 $M_\odot$.
- These are not expected to form as the endpoint of stellar evolution.

[Wyrzykowski & Mandel 2020]

Quasar Microlensing

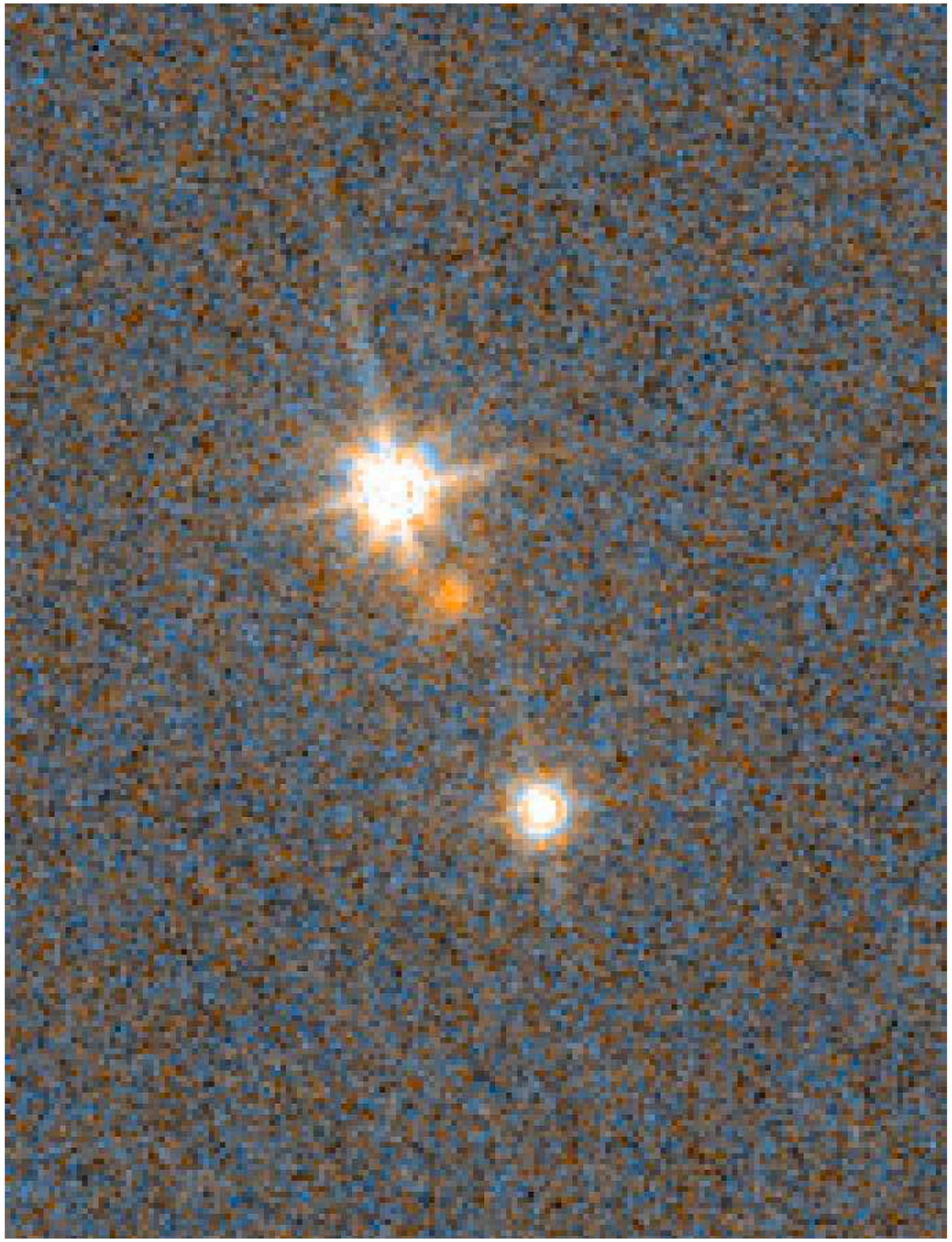

HST image of lensed quasar HE1104–1805

The signature of primordial black holes in the dark matter halos of galaxies

M. R. S. Hawkins

Institute for Astronomy (IfA), University of Edinburgh, Royal Observatory, Blackford Hill, Edinburgh EH9 3HJ, UK
e-mail: mrsh@roe.ac.uk

ABSTRACT

Aims. The aim of this paper is to investigate the claim that stars in the lensing galaxy of a gravitationally lensed quasar system can always account for the observed microlensing of the individual quasar images. [...]
Results. Taken together, the probability that all the observed microlensing is due to stars was found to be $\sim 3 \times 10^{-4}$. Errors resulting from the surface brightness measurement, the mass-to-light ratio, and the contribution of the dark matter halo do not significantly affect this result.
Conclusions. It is argued that the most plausible candidates for the microlenses are primordial black holes, either in the dark matter halos of the lensing galaxies, or more generally distributed along the lines of sight to the quasars.

Calcium-Rich Gap Transients

★ A supernova population of so-called calcium-rich gap transients has been shown to clearly not to follow the stellar distribution but rather a would-be compact dark matter one.

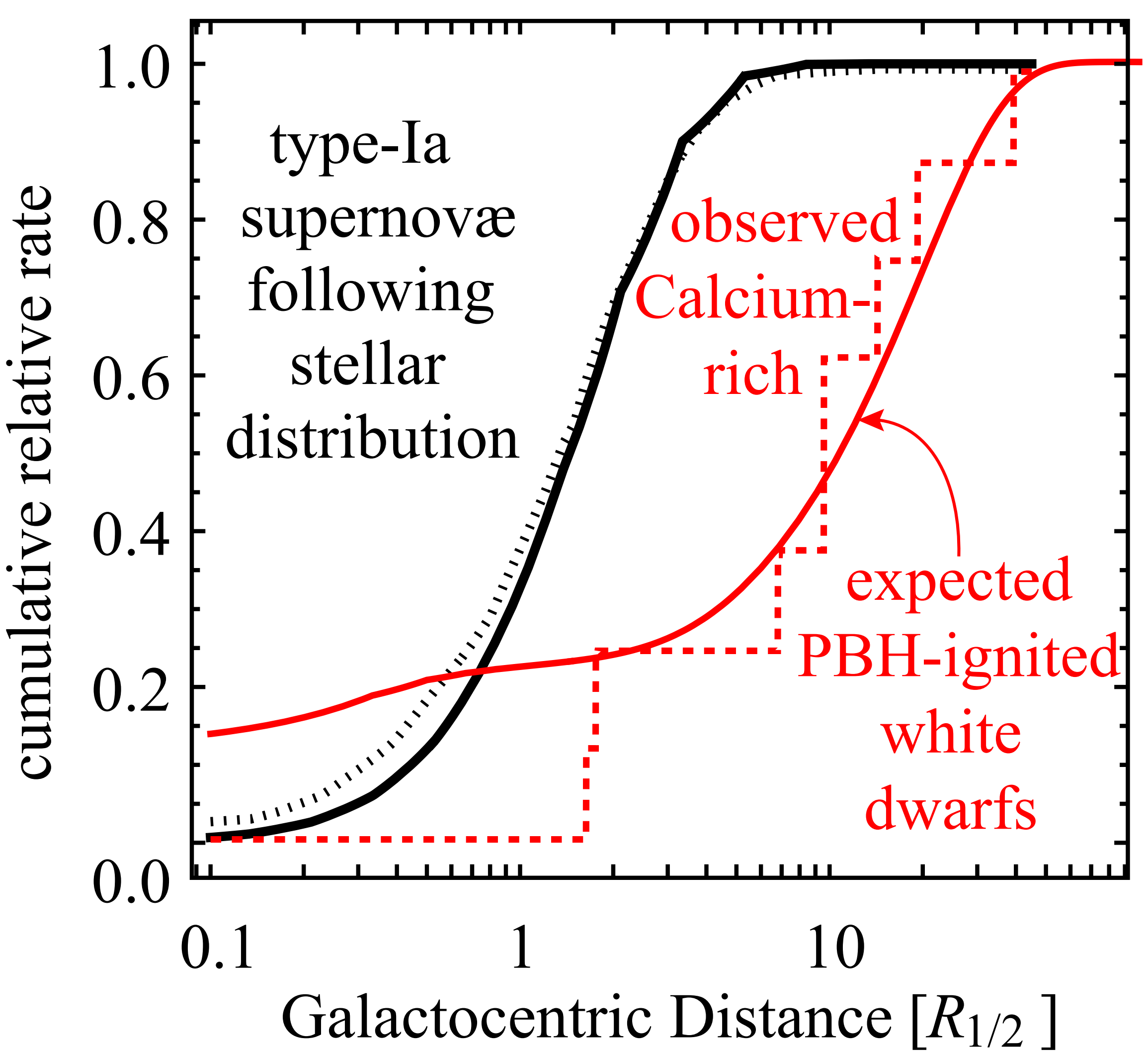

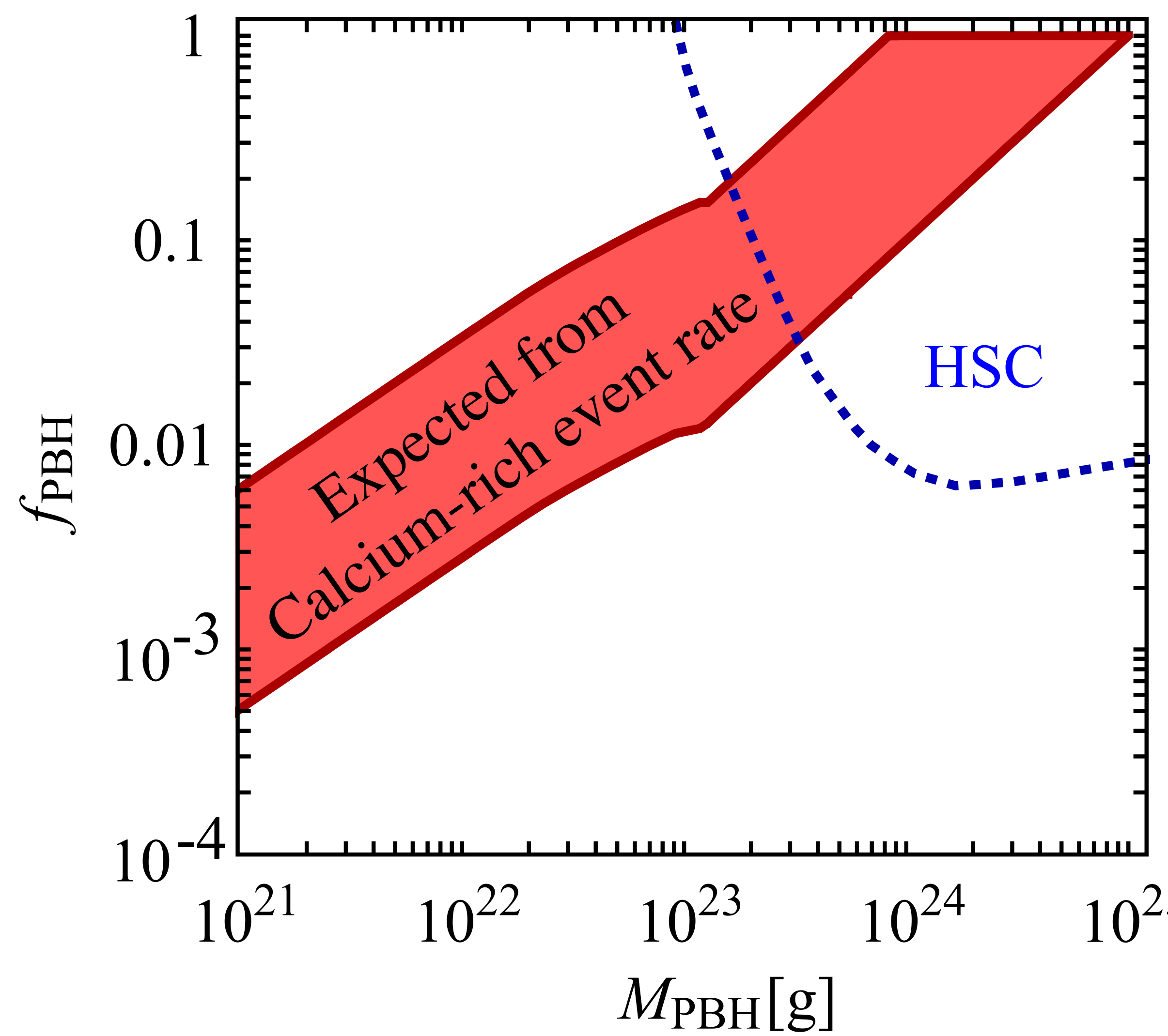

[Smirnov *et al.* 2023]

Correlations of Cosmic Infrared/X-Ray Backgrounds

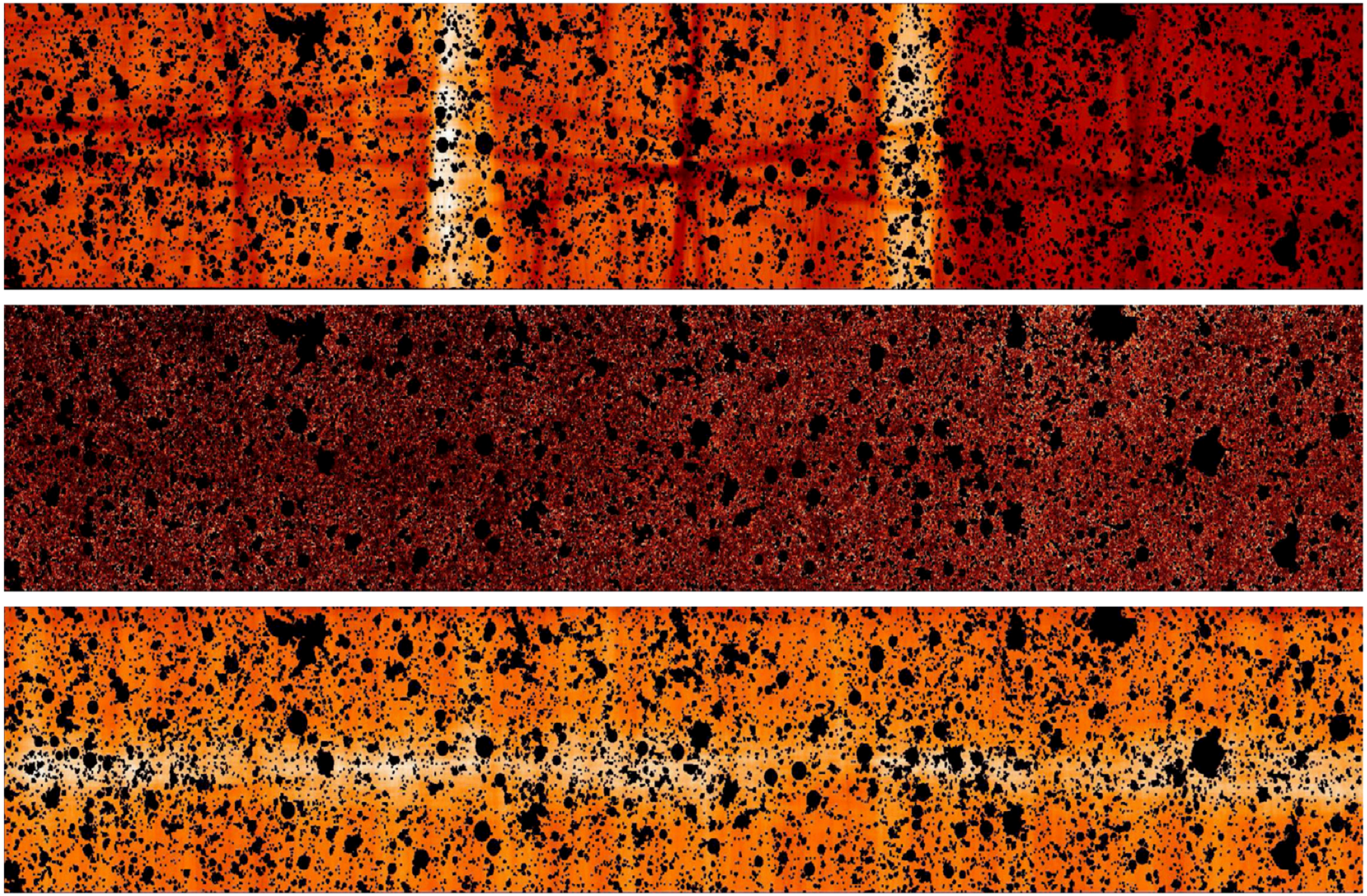

[Cappelluti *et al.* 2013]

★ PBHs generate early structure and respective backgrounds

Ultra-faint Dwarf Galaxies

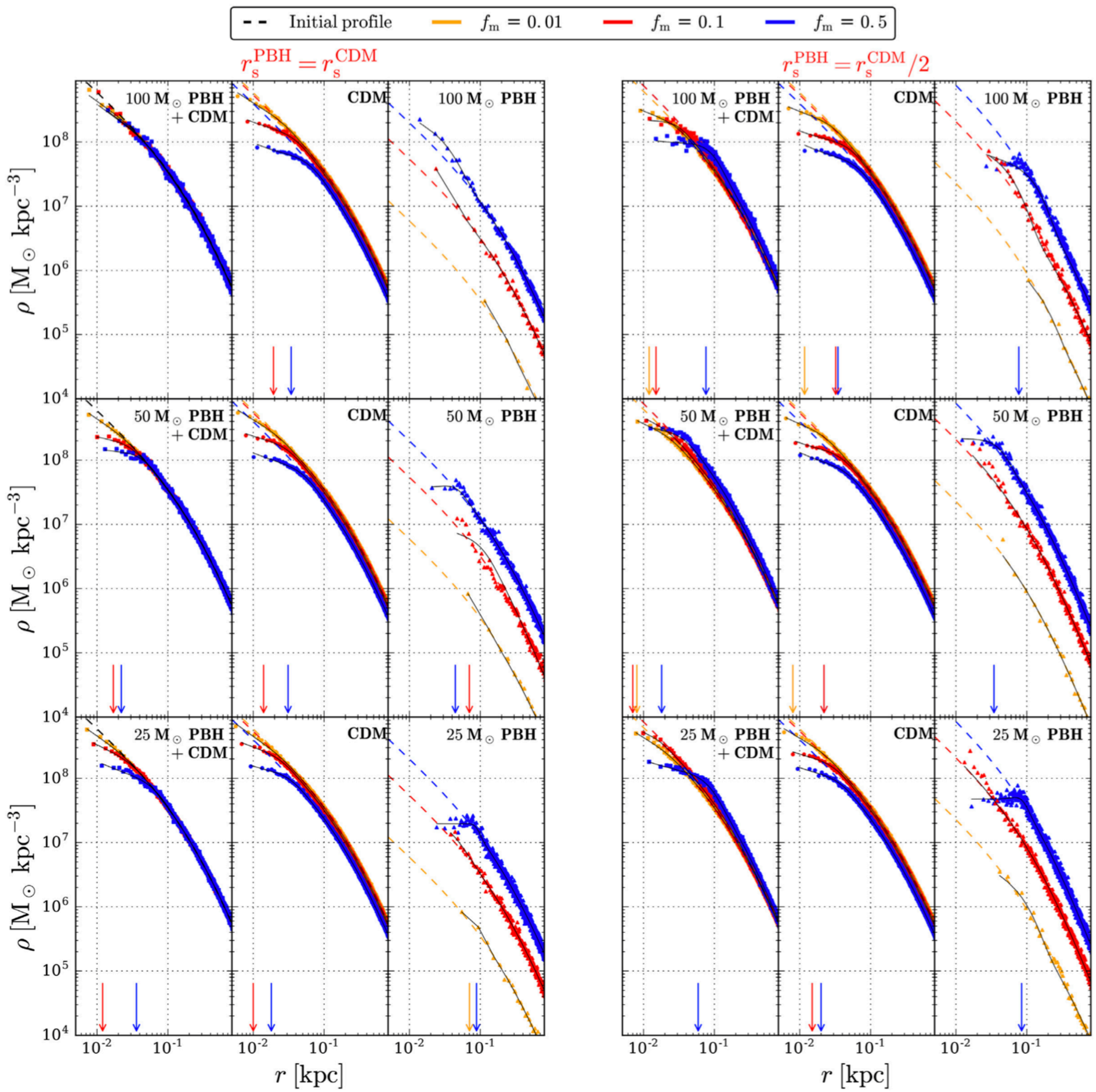

[Boldrini *et al.* 2020]

★ Non-detection of dwarf galaxies smaller than ~ 10 – 20 pc

★ Ultra-faint dwarf galaxies are dynamically unstable below some critical radius in the presence of PBH CDM!

★ This works with a few percent of PBH DM of 25 – 100 $M_\odot$.

GRAVITATIONAL WAVE **MERGER** DETECTIONS

SINCE 2015

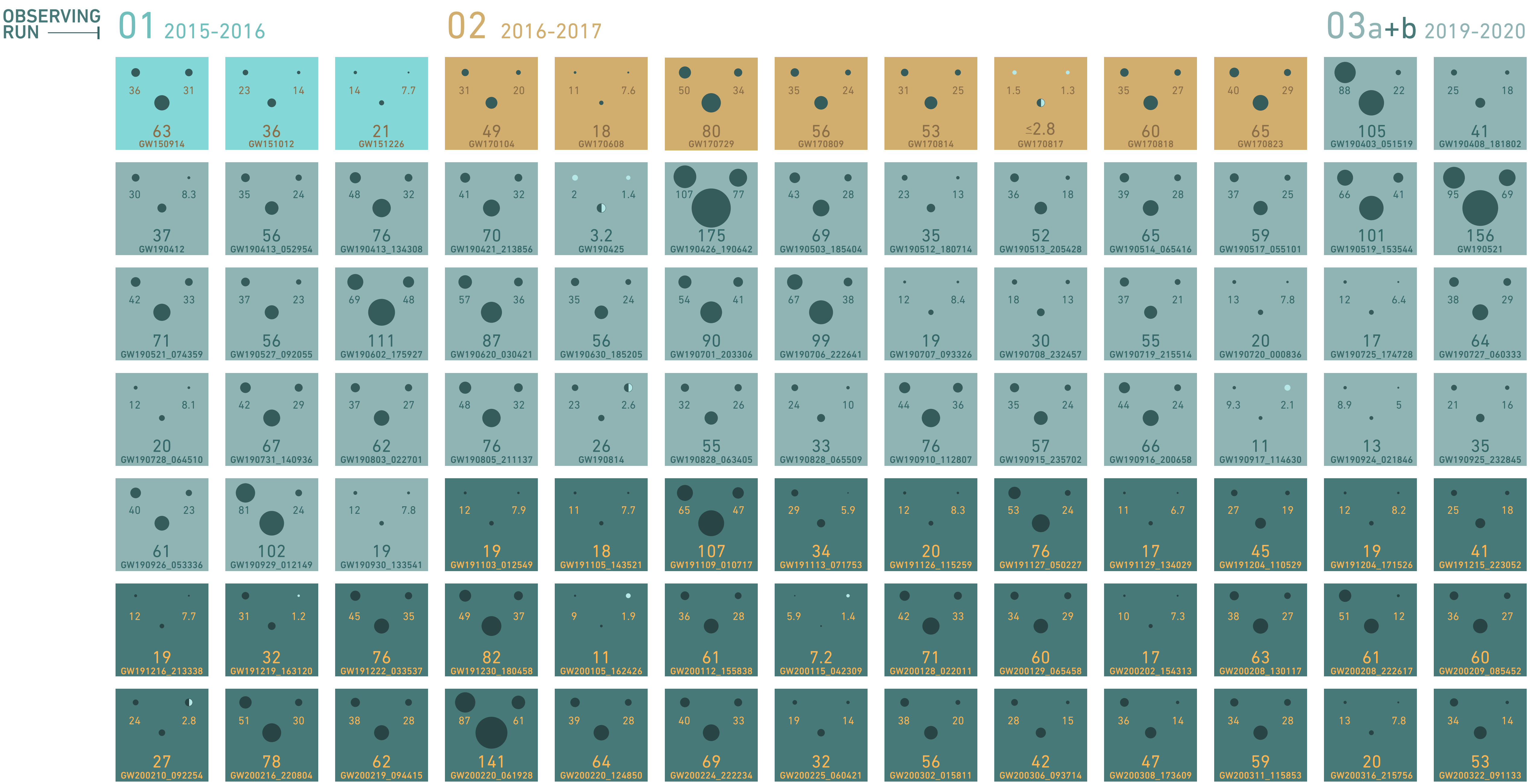

LIGO VIRGO KAGRA

GRAVITATIONAL WAVE **MERGER** DETECTIONS

SINCE 2015

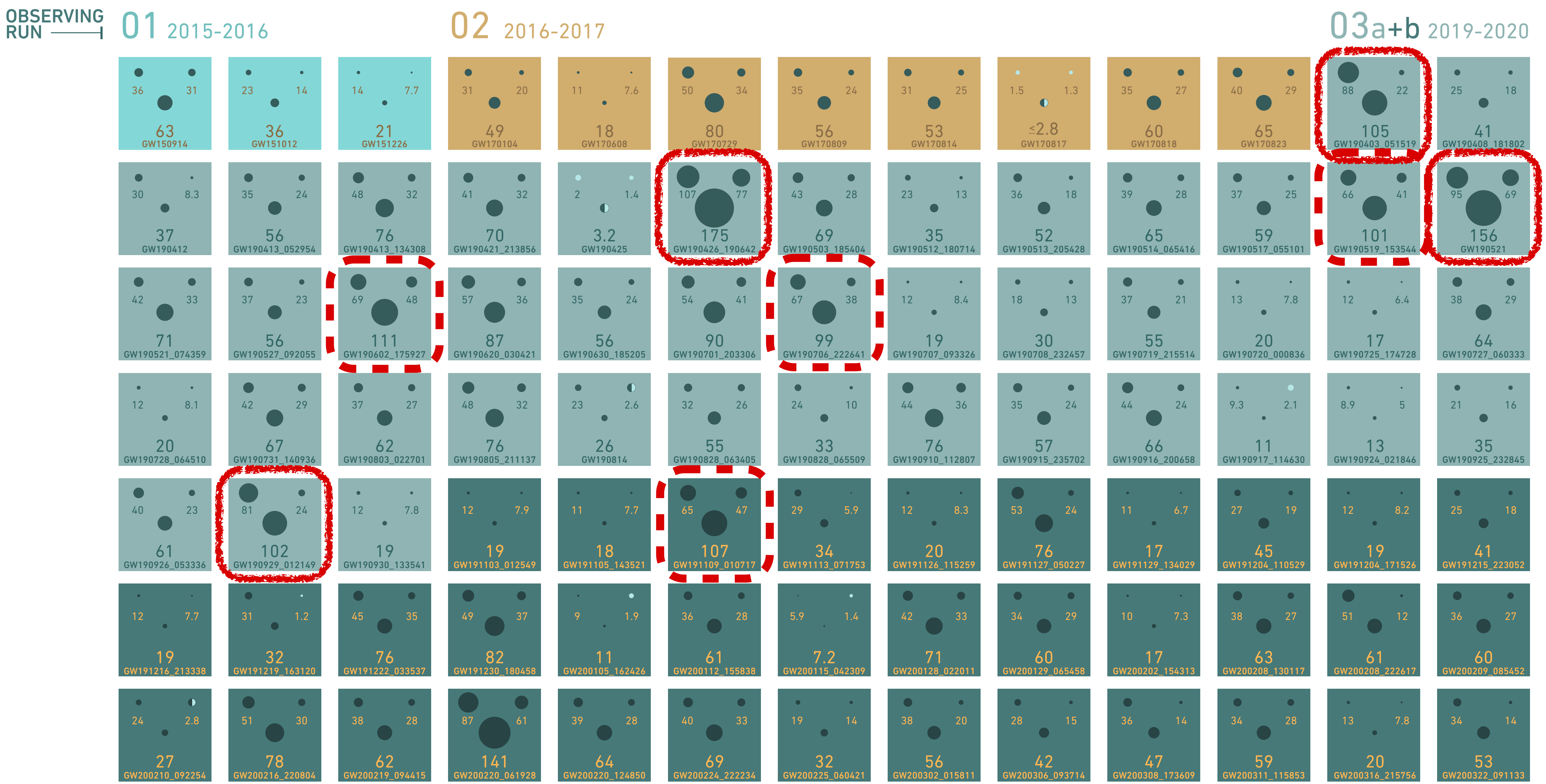

★ Black hole progenitors in the pair-instability mass gap (i.e. above ~ 60 $M_\odot$)

GRAVITATIONAL WAVE **MERGER** DETECTIONS

SINCE 2015

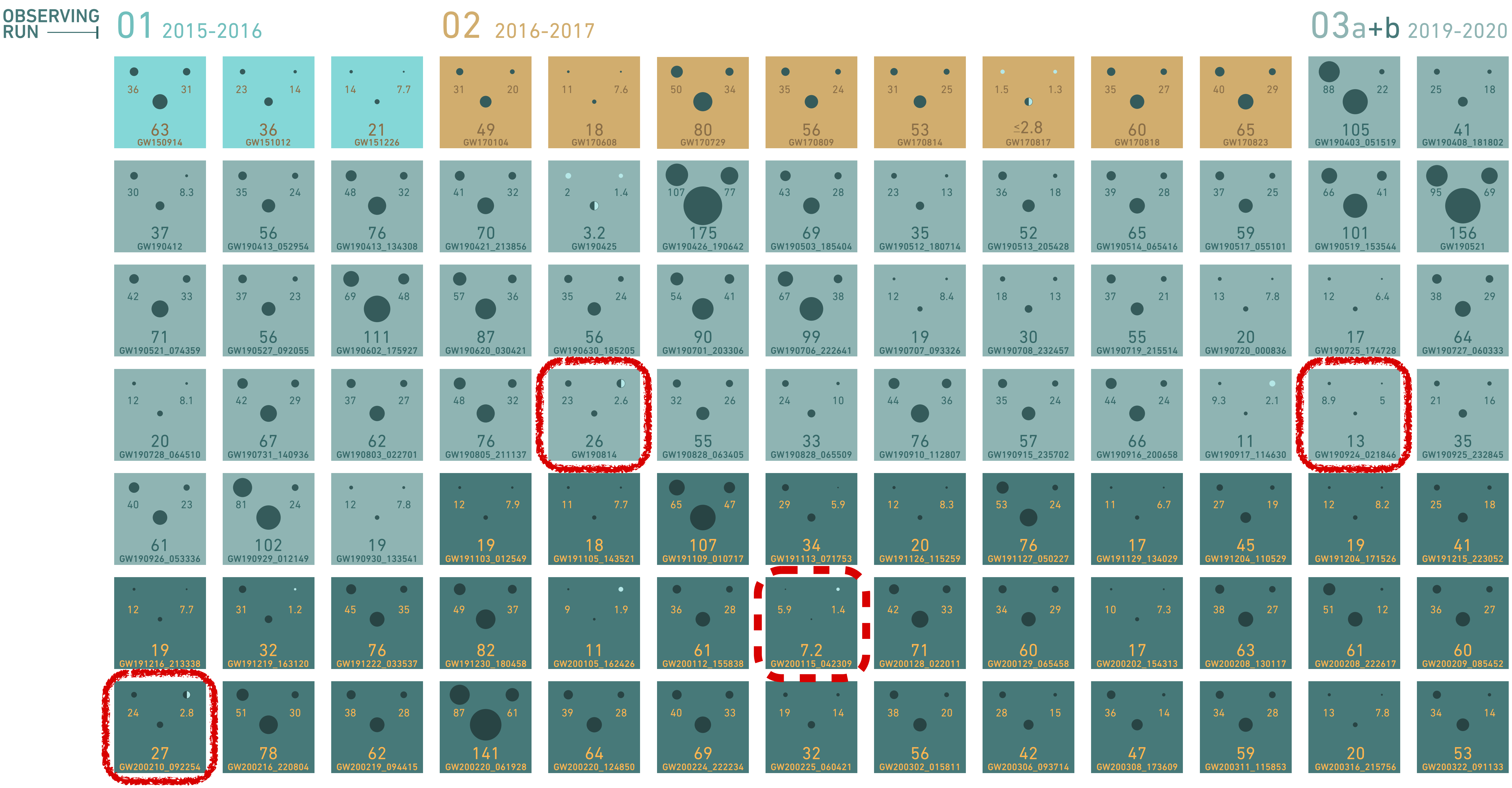

★ Black hole progenitors in the lower mass gap (i.e. between 2 and 5 $M_\odot$)

LIGO VIRGO KAGRA

GRAVITATIONAL WAVE **MERGER** DETECTIONS

SINCE 2015

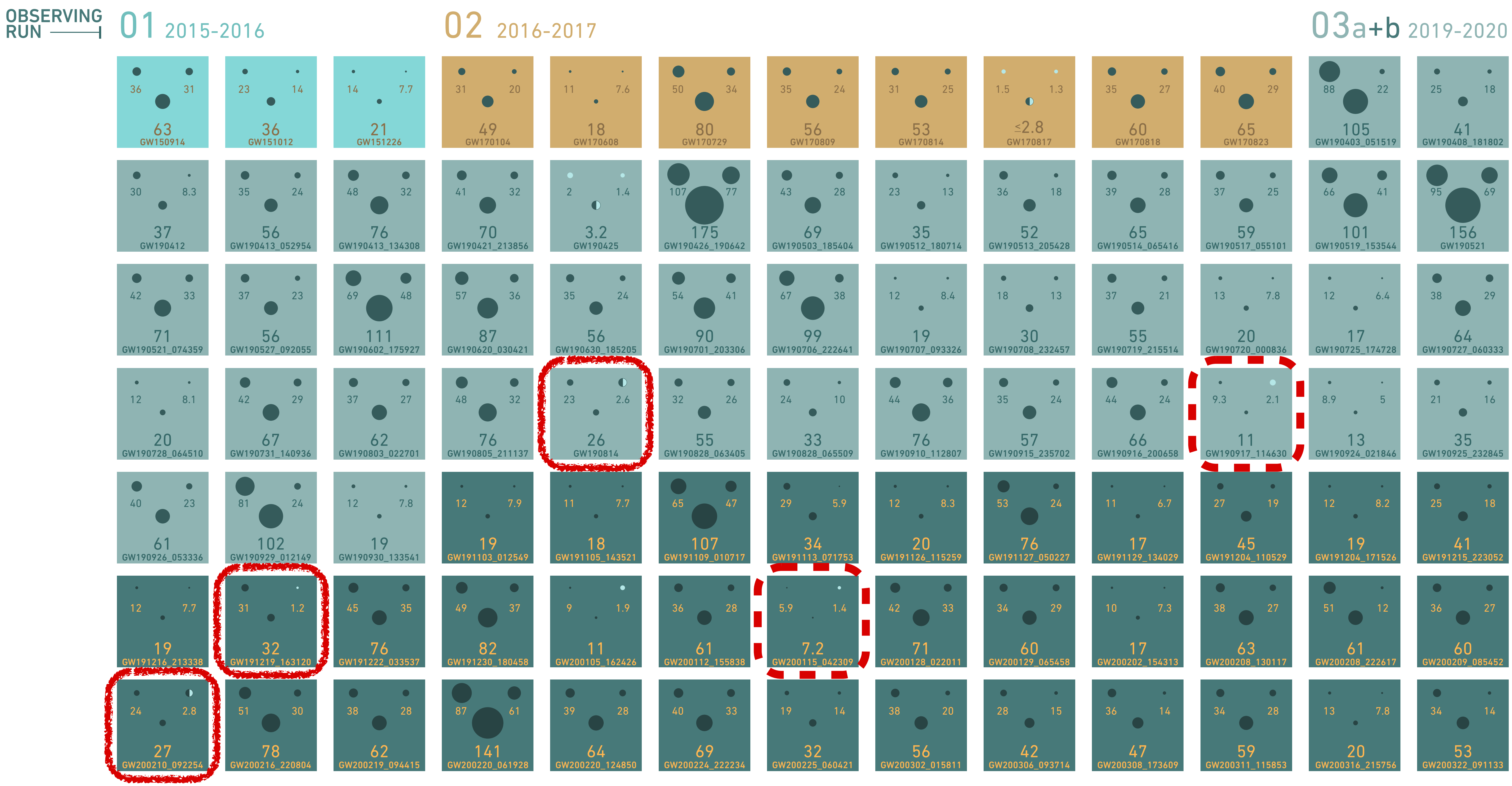

★ Asymmetric black hole progenitors (mass ratio $q < 0.25$)

GRAVITATIONAL WAVE **MERGER** DETECTIONS

SINCE 2015

The Astrophysical Journal Letters, 896:L44 (20pp), 2020 June 20 https://doi.org/10.3847/2041-8213/ab960f

GW190814: Gravitational Waves from the Coalescence of a 23 Solar Mass Black Hole with a 2.6 Solar Mass Compact Object

R. Abbott[1], [...]

Abstract

We report the observation of a compact binary coalescence involving a 22.2–24.3 $M_\odot$ black hole and a compact object with a mass of 2.50–2.67 $M_\odot$ [...] the combination of mass ratio, component masses, and the inferred merger rate for this event challenges all current models of the formation and mass distribution of compact-object binaries.

★ Asymmetric black hole progenitors (mass ratio $q < 0.25$)

LIGO VIRGO KAGRA

Subsolar Black Holes - The Smoking Gun!

- Recent reanalysis of LIGO data updated merger rates and low mass ratios:

Date	FAR [yr^{-1}]	$m_1[M_\odot]$	$m_2[M_\odot]$	spin-1-z	spin-2-z	H SNR	L SNR	V SNR	Network SNR
2017-04-01	0.41	4.90	0.78	−0.05	−0.05	6.32	5.94	–	8.67
2017-03-08	1.21	2.26	0.70	−0.04	−0.04	6.32	5.74	–	8.54
2020-03-08	0.20	0.78	0.23	0.57	0.02	6.31	6.28	-	8.90
2019-11-30	1.37	0.40	0.24	0.10	−0.05	6.57	5.31	5.81	10.25
2020-02-03	1.56	1.52	0.37	0.49	0.10	6.74	6.10	-	9.10

- Five strong subsolar candidates with SNR > 8 and a FAR < 2 yr^{-1}

- Possibly the first confirmed detection of a subsolar mass PBH with the next 12 months!

Further Reasons for PBHs

- Primordial black holes could furthermore explain
  - high-redshift galaxy candidates (up to $z = 16$!)
  - MACHO microlensing results
  - Seeds for supermassive black holes
  - fast radio bursts
  - missing pulsars
  - ...

A Unified Scenario

Thermal History of the Universe — Degrees of Freedom

★ Changes in the relativistic degrees of freedom:

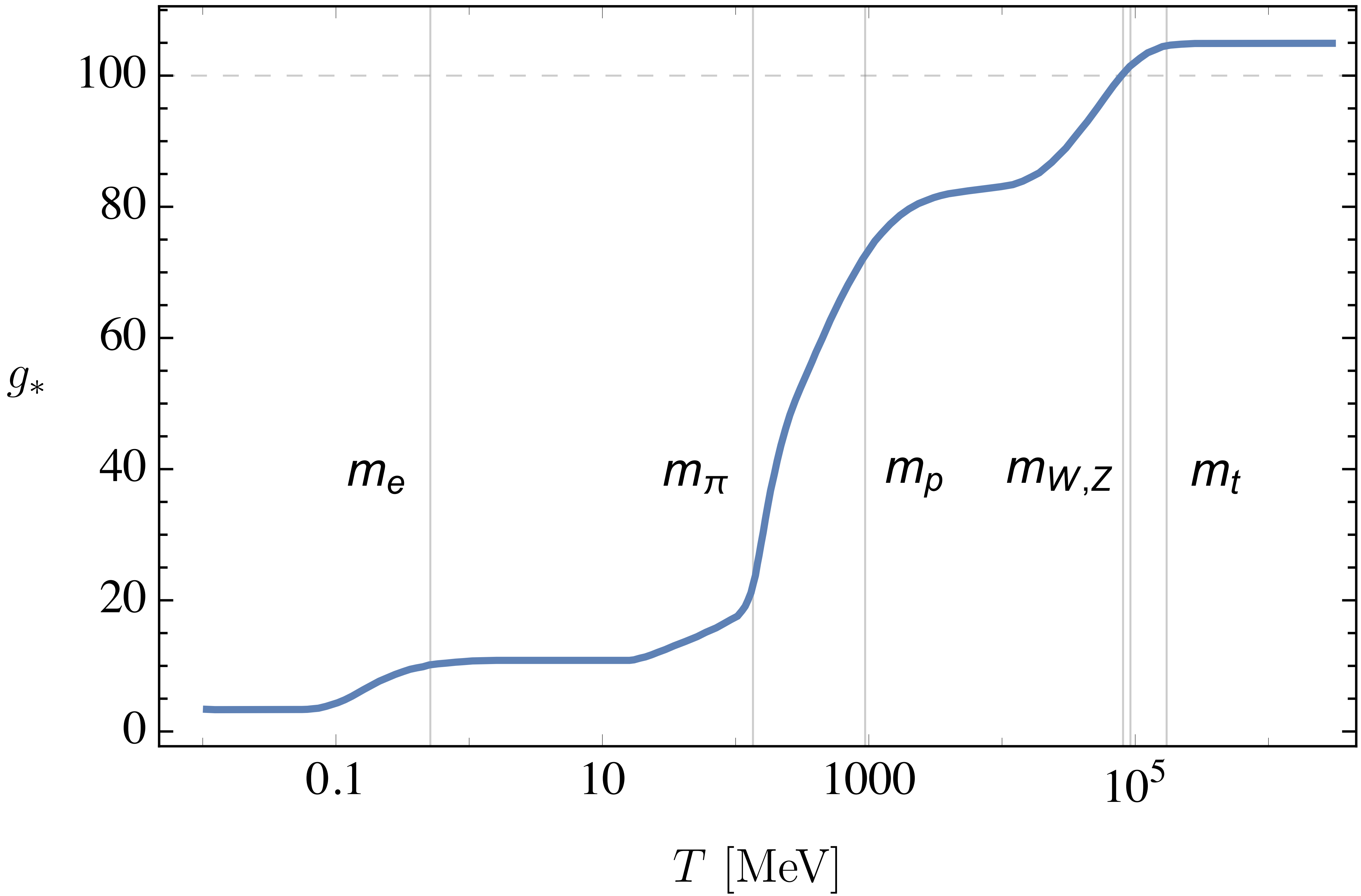

Thermal History of the Universe — Equation of State

★ Changes in the equation-of-state parameter $w = p/\rho$:

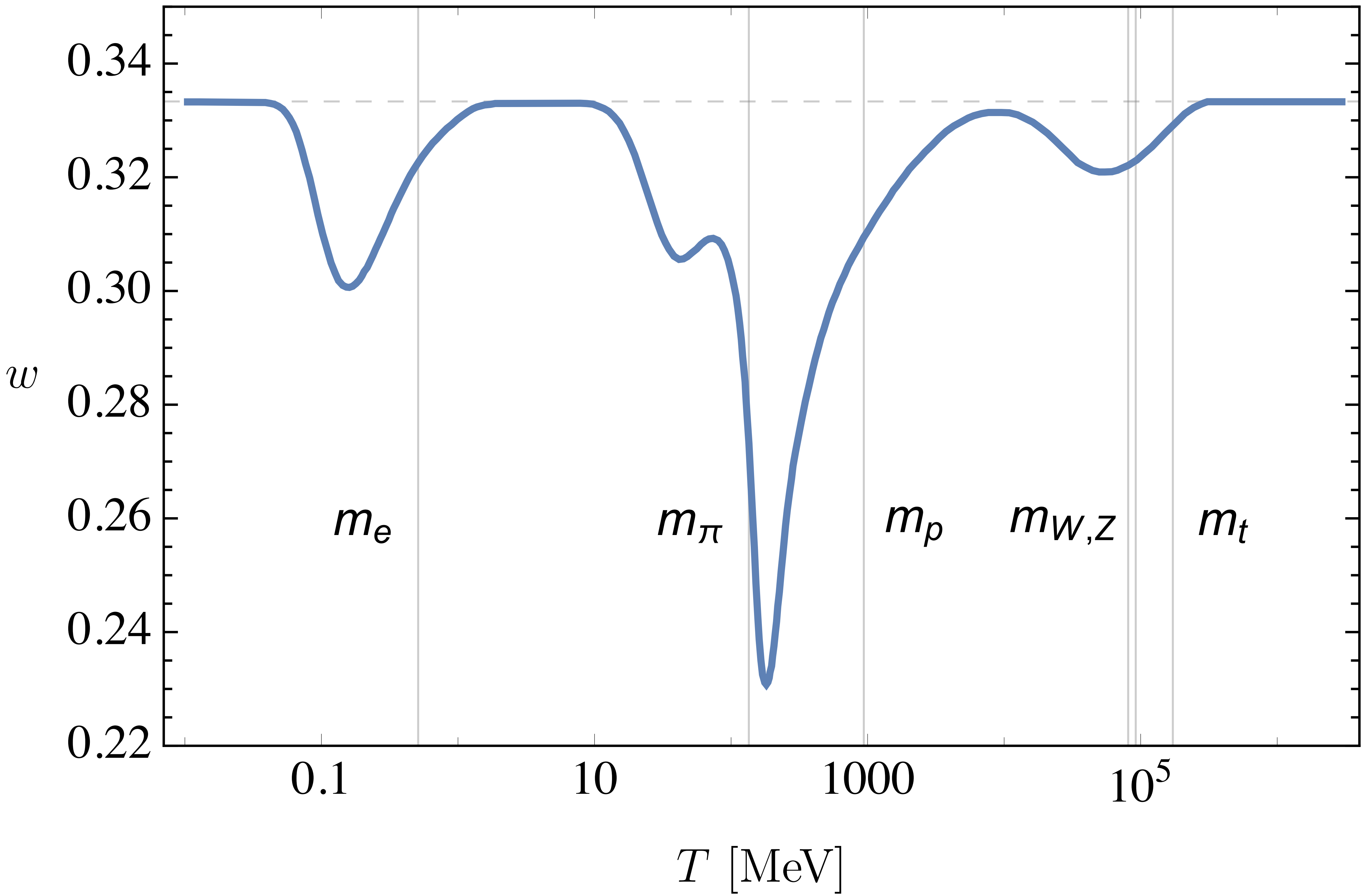

Primordial Power Spectrum — Planck to PBH

★ Consider an essentially featureless power spectrum:

$$\mathcal{P}(k) \sim k^{n_s - 1 + \frac{1}{2}\alpha_s \ln(k/k_*)}$$

as suggested by Planck, albeit on *large non-PBH scales*...

★ Connection to *small PBH scales* for instance by critical Higgs inflation.

[García-Bellido, Ruiz-Morales 2017]

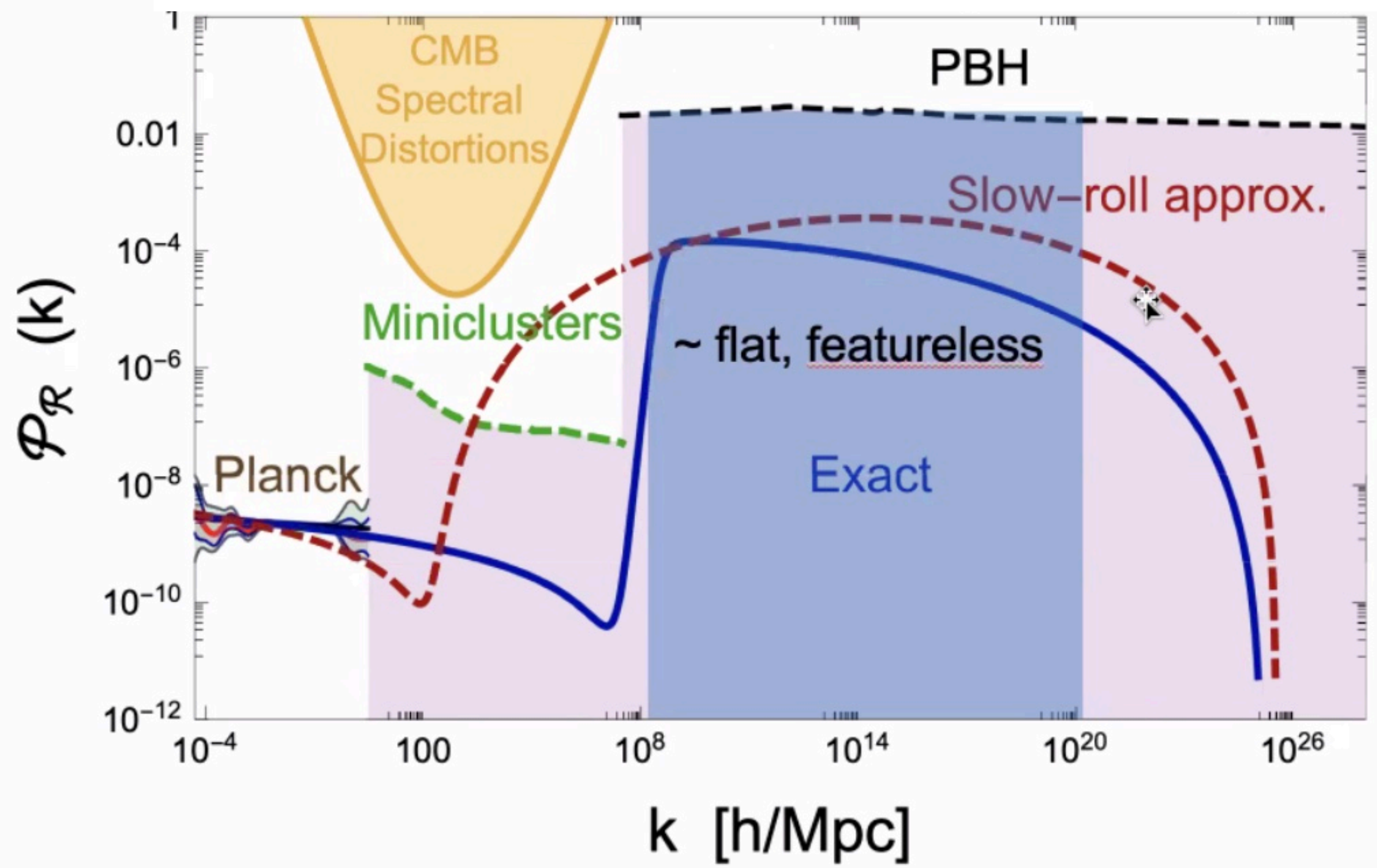

Figure from García-Bellido

PBH Mass Function

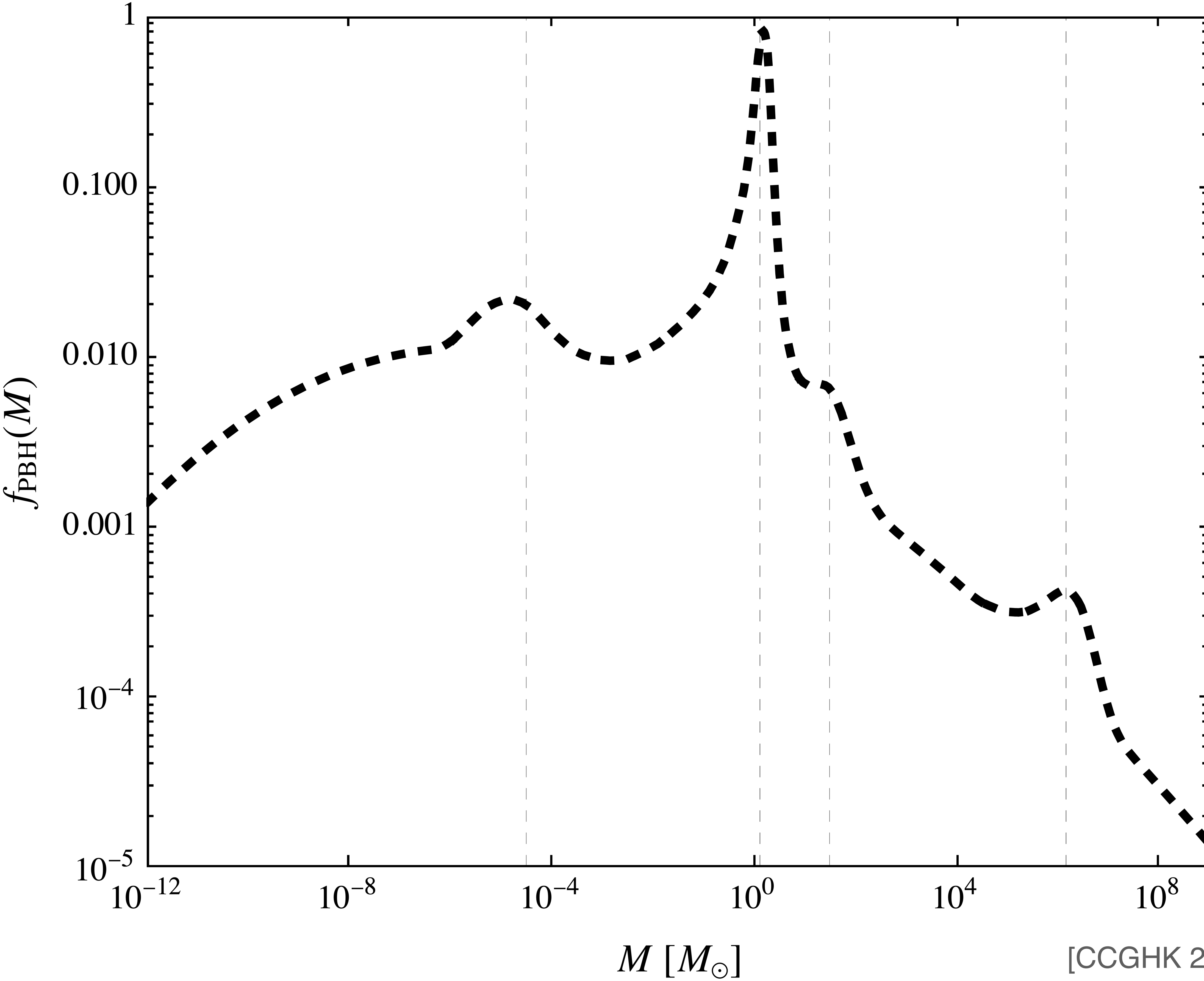

[CCGHK 2023]

PBH Mass Function

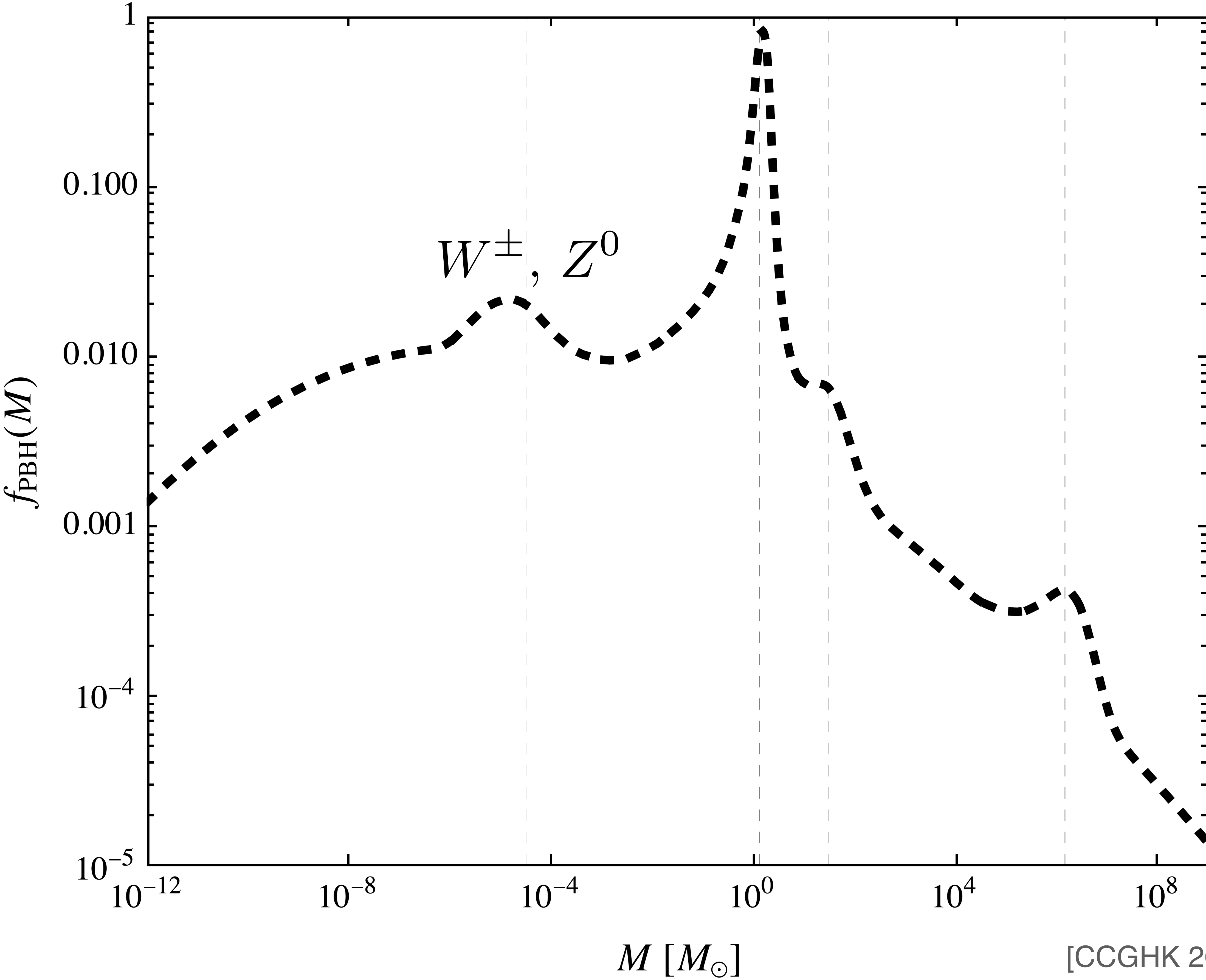

[CCGHK 2023]

PBH Mass Function

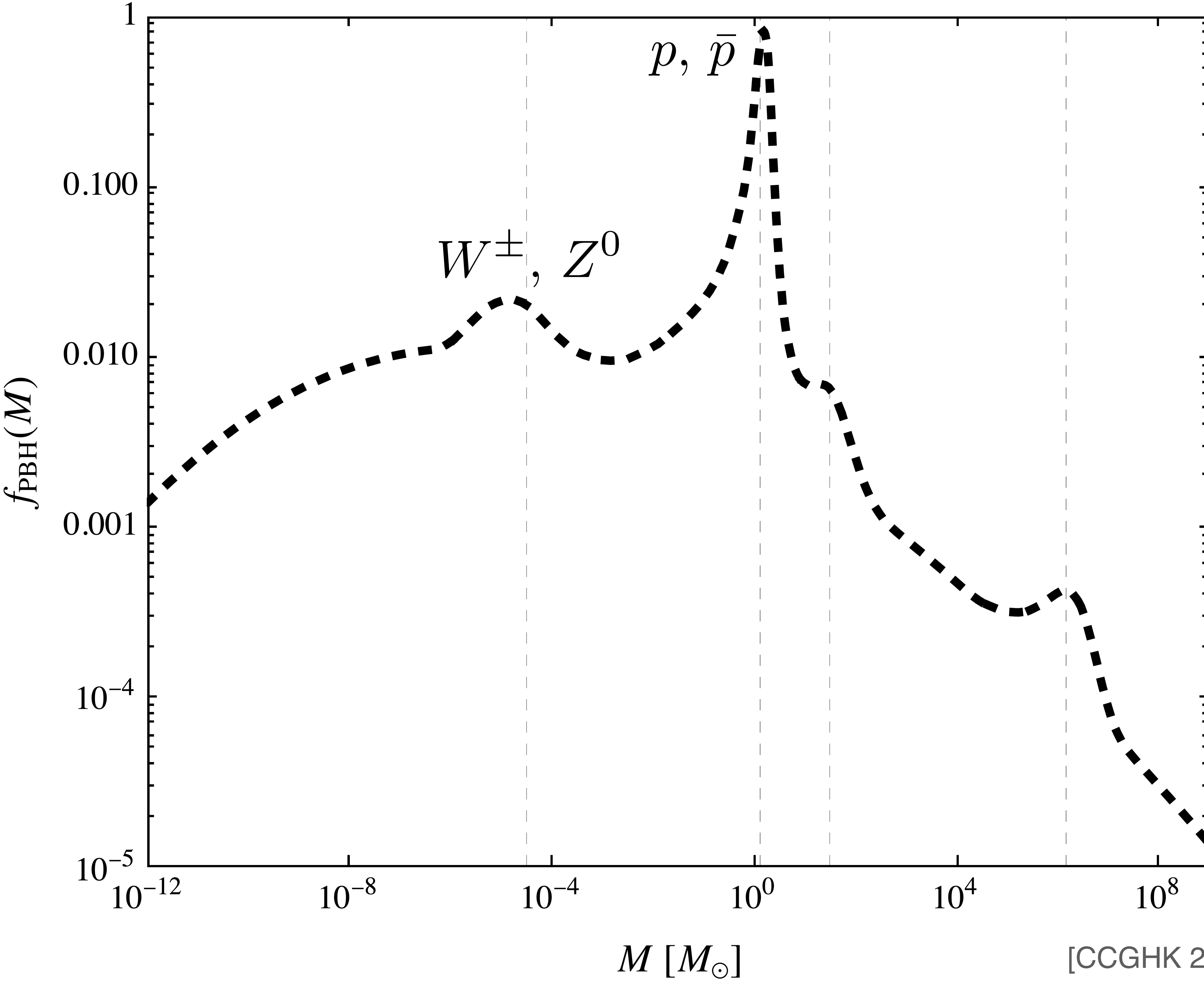

[CCGHK 2023]

PBH Mass Function

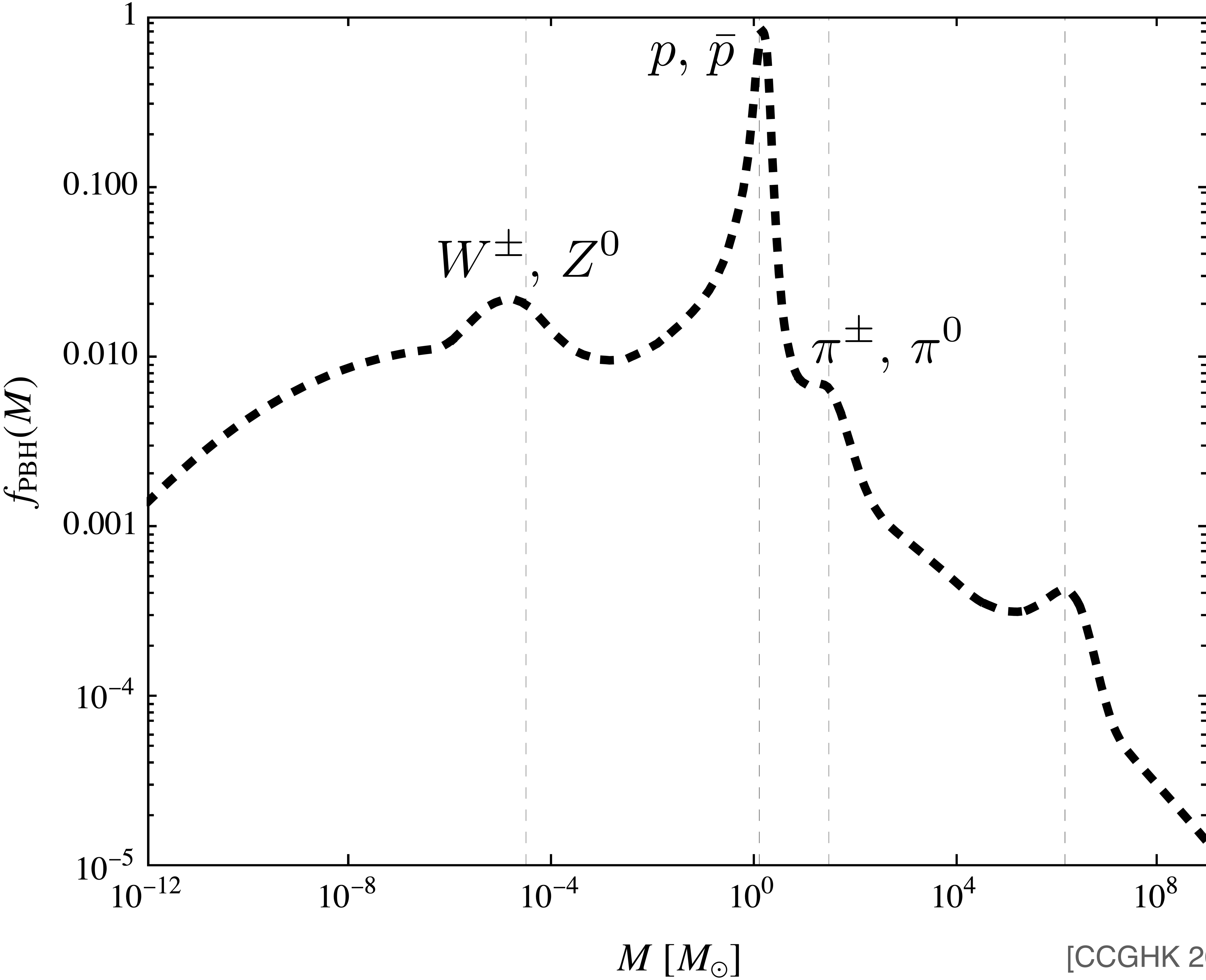

[CCGHK 2023]

PBH Mass Function

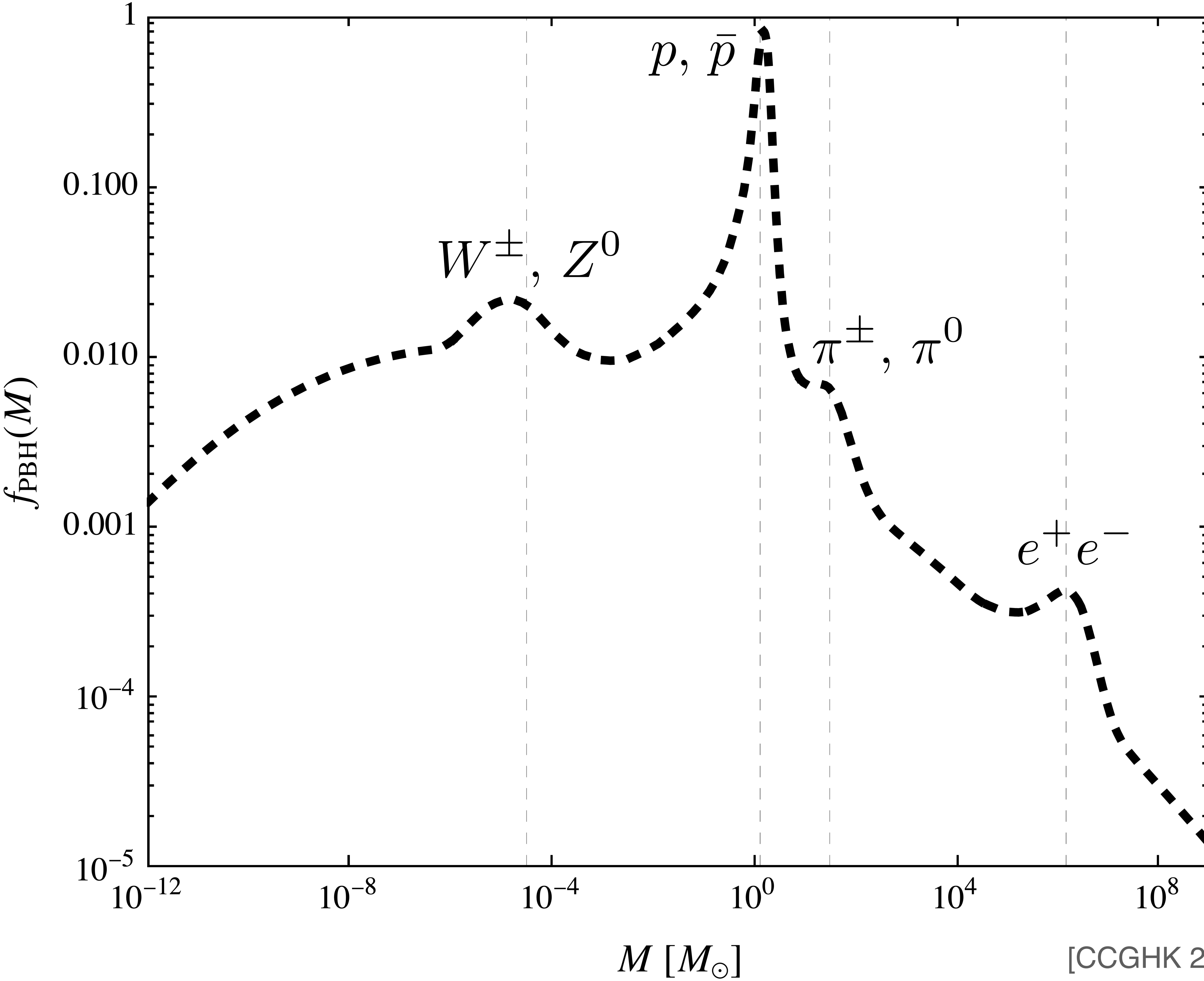

[CCGHK 2023]

PBH Mass Function

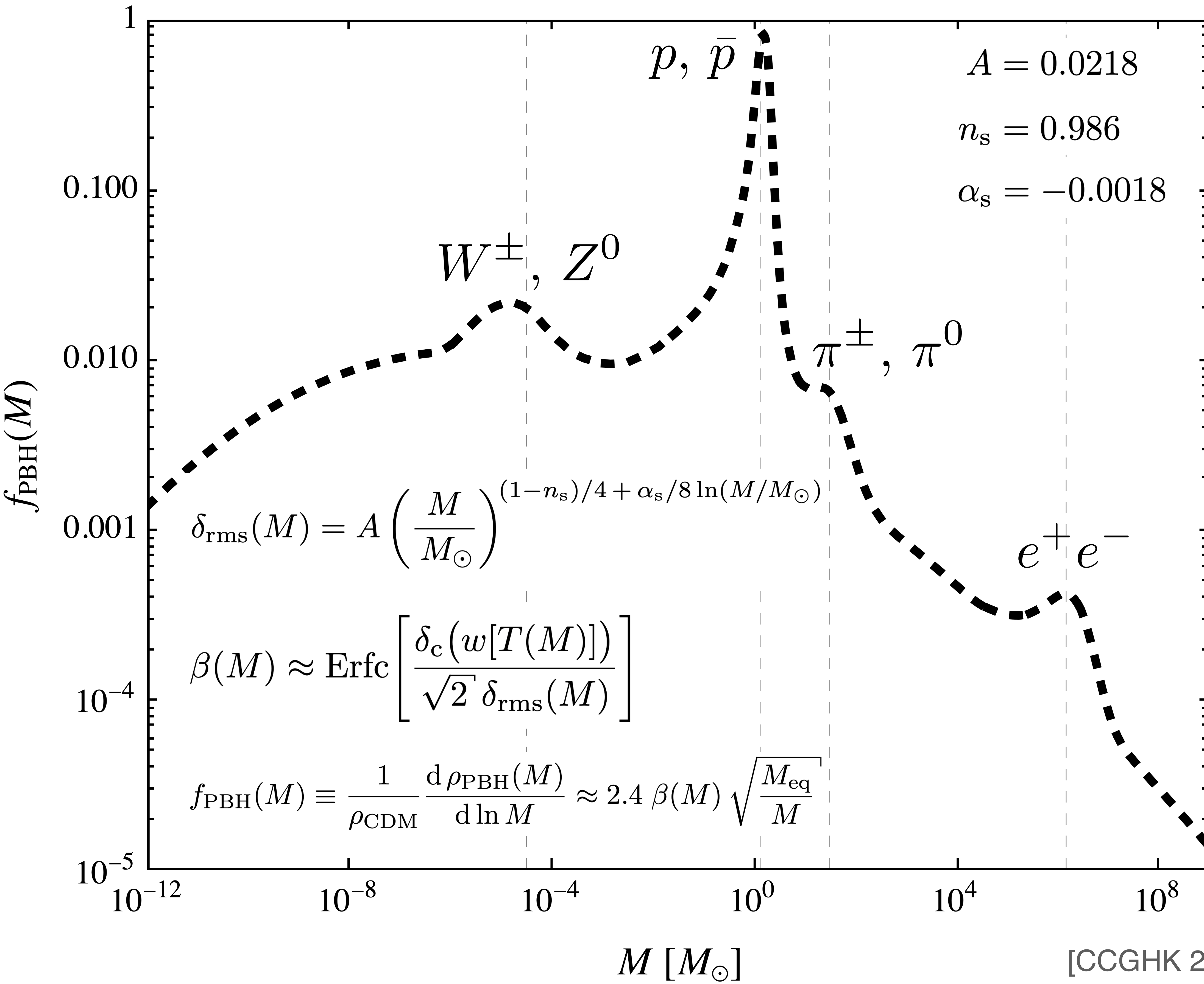

[CCGHK 2023]

PBH Mass Function

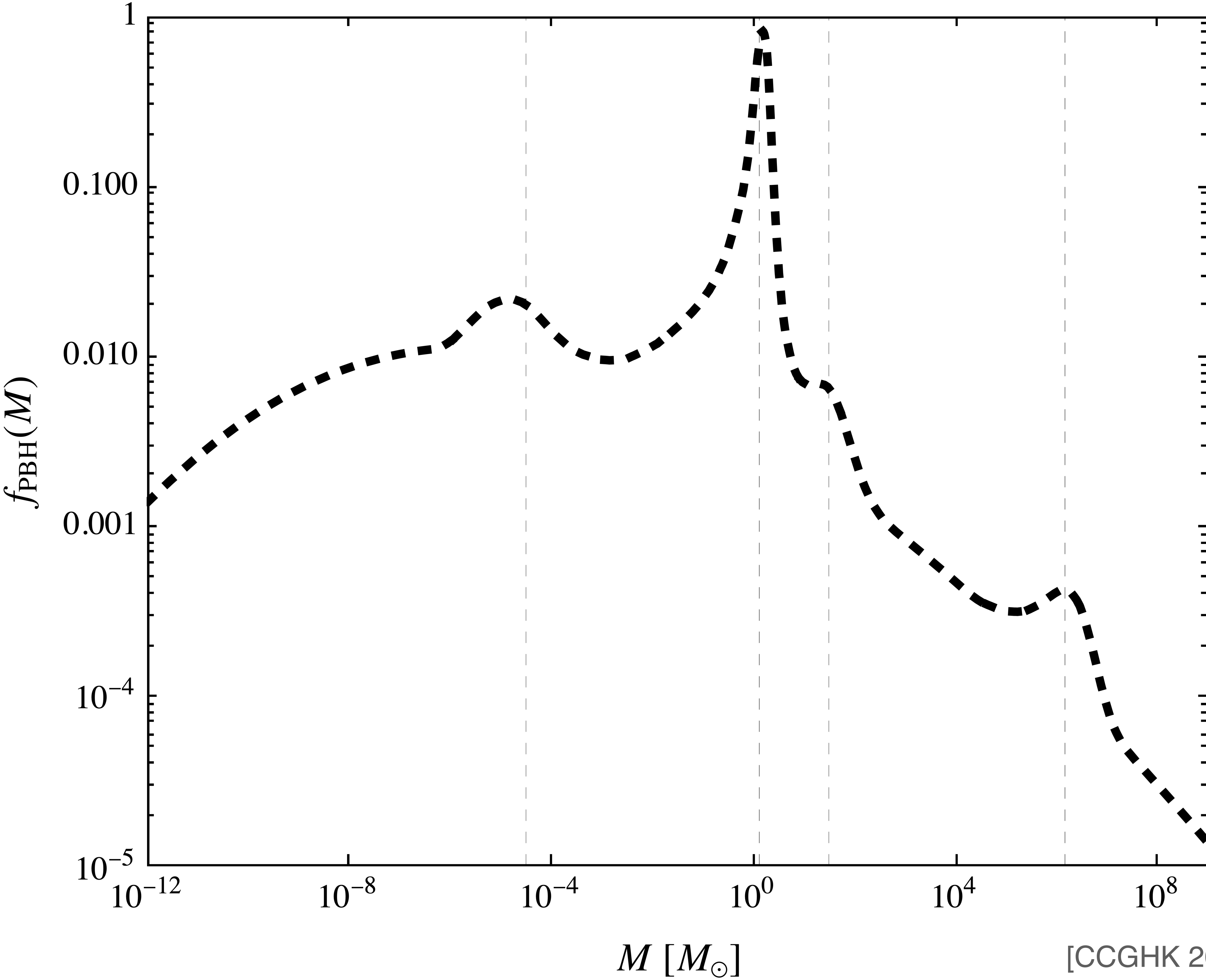

[CCGHK 2023]

PBH Mass Function — Confronted with Observations

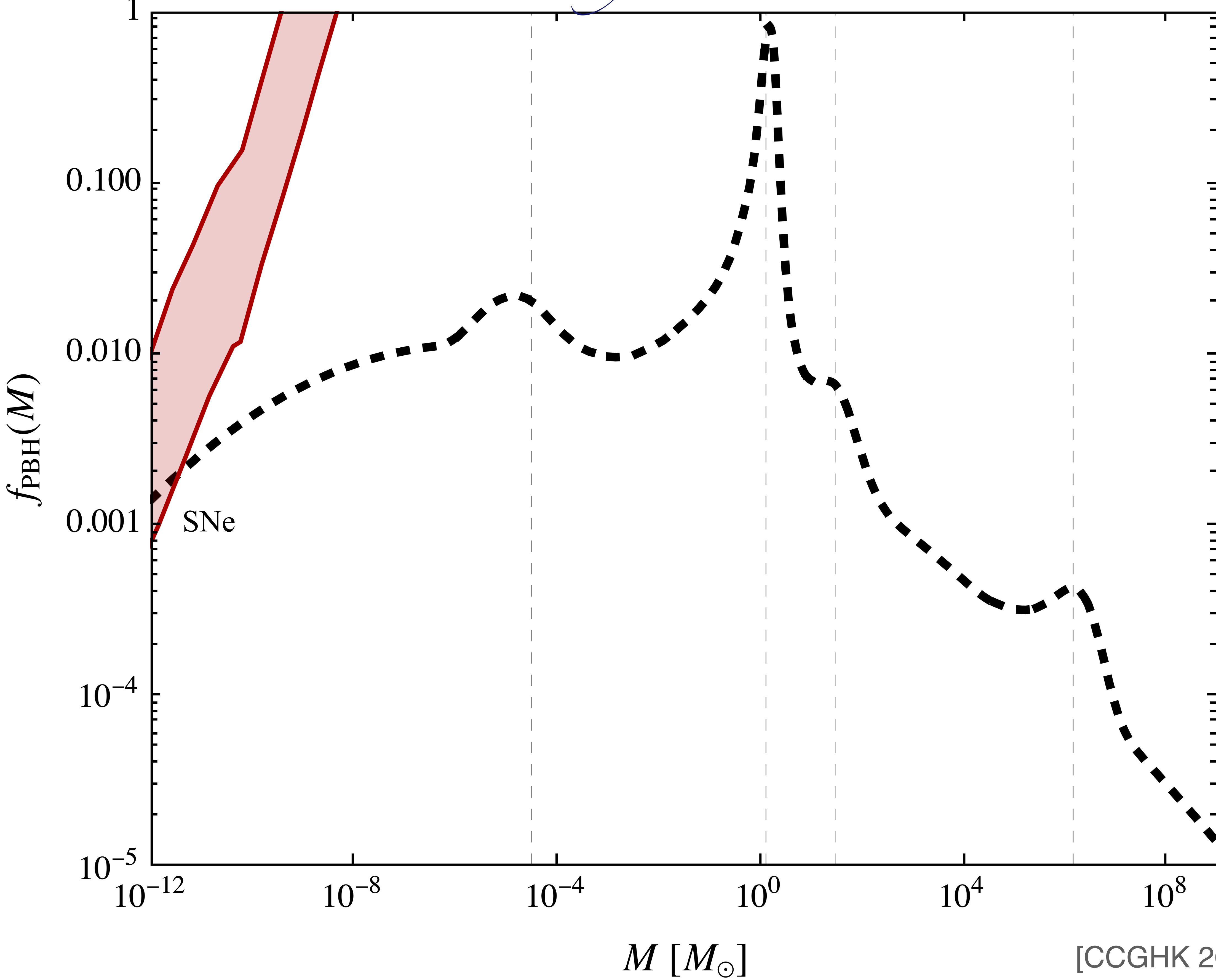

[CCGHK 2023]

PBH Mass Function — Confronted with Observations

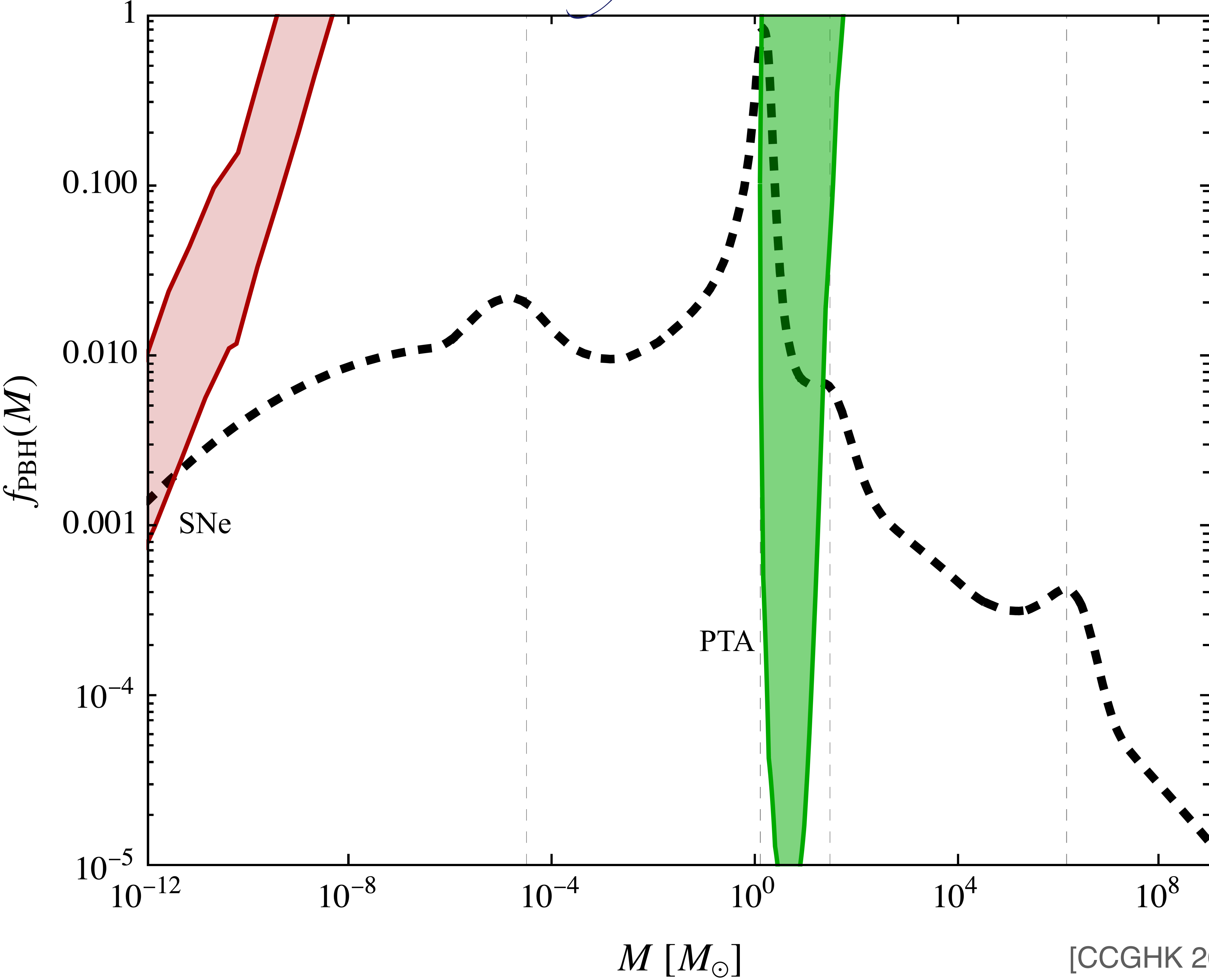

[CCGHK 2023]

PBH Mass Function — Confronted with Observations

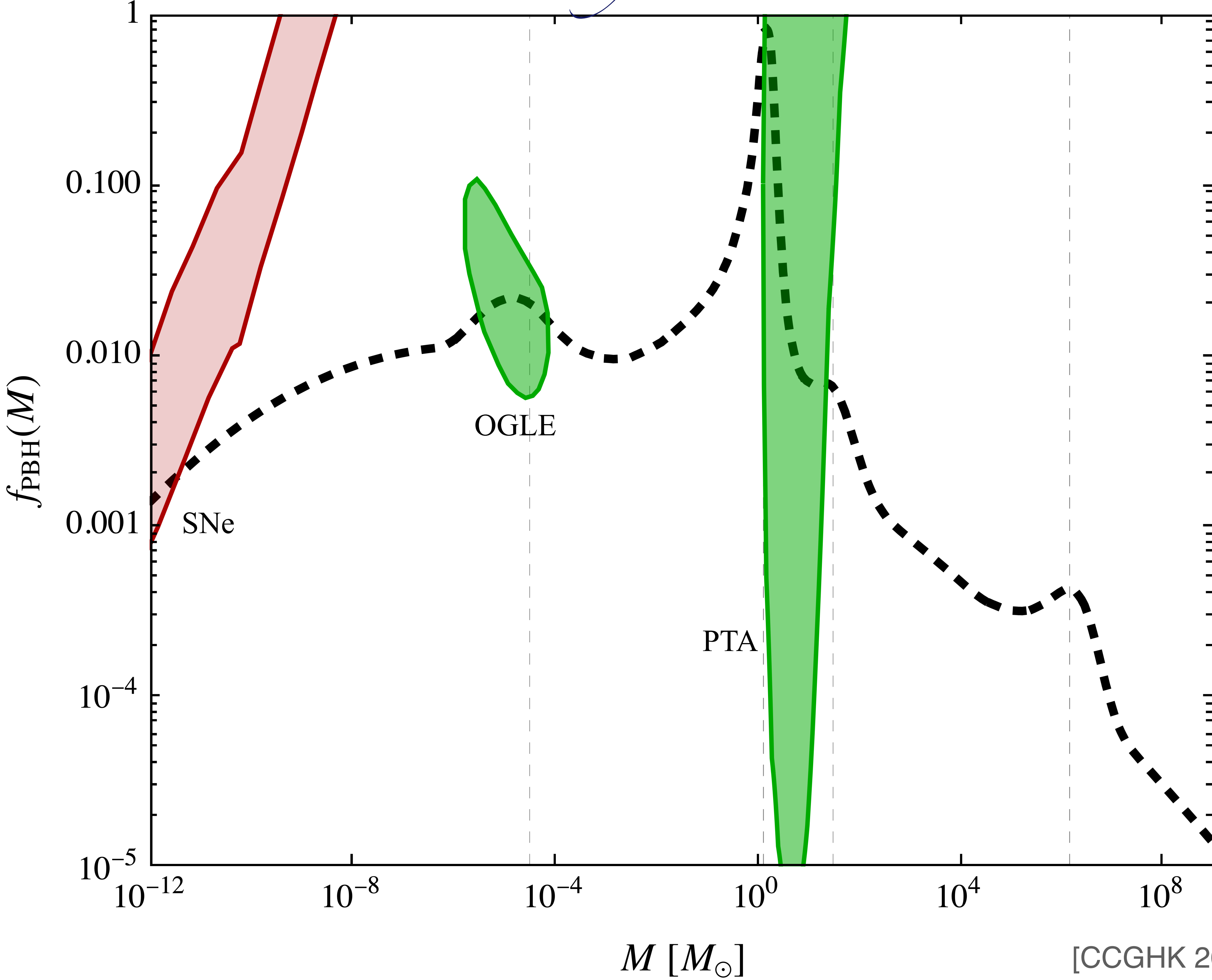

[CCGHK 2023]

PBH Mass Function — Confronted with Observations

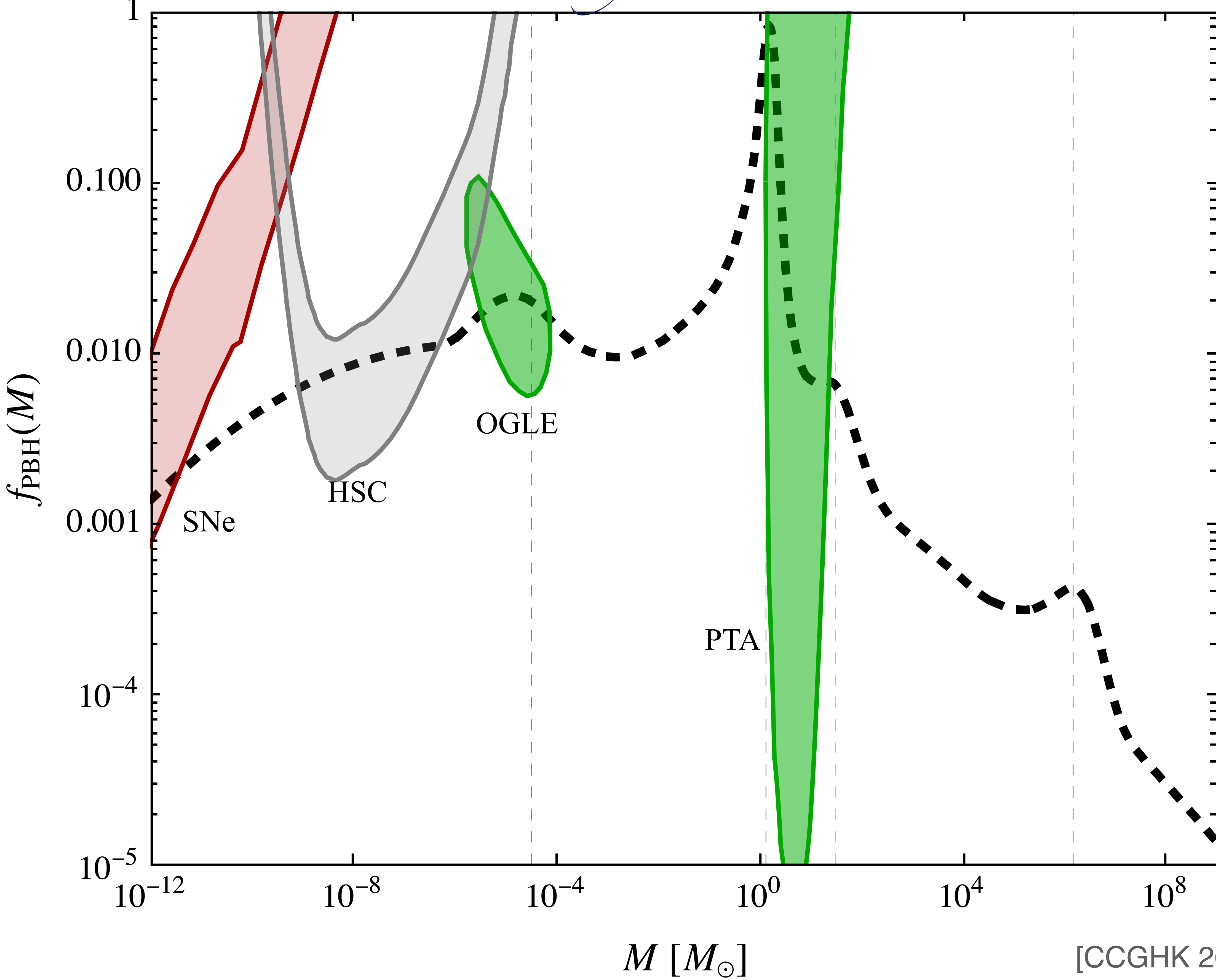

[CCGHK 2023]

PBH Mass Function — Confronted with Observations

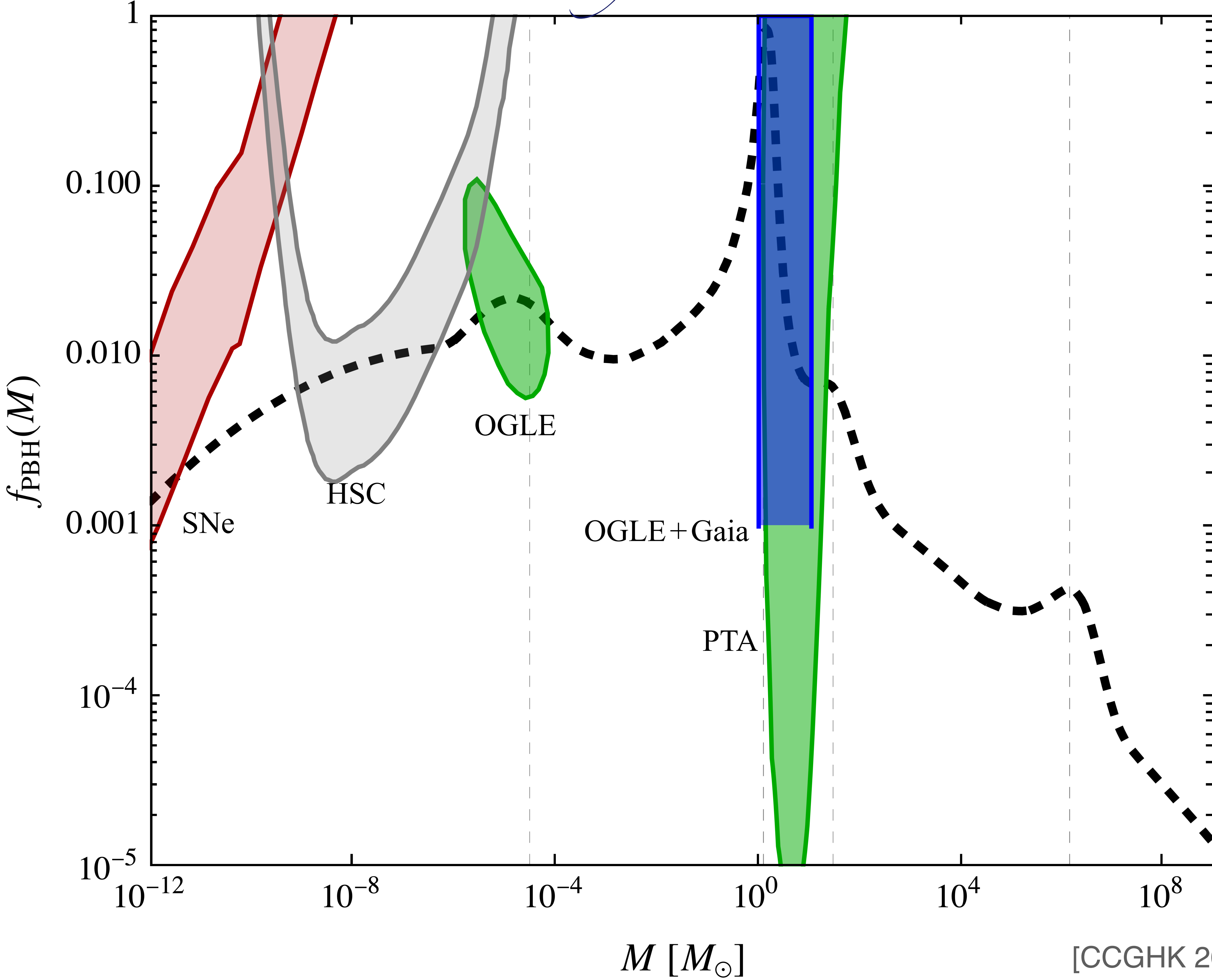

[CCGHK 2023]

PBH Mass Function — Confronted with Observations

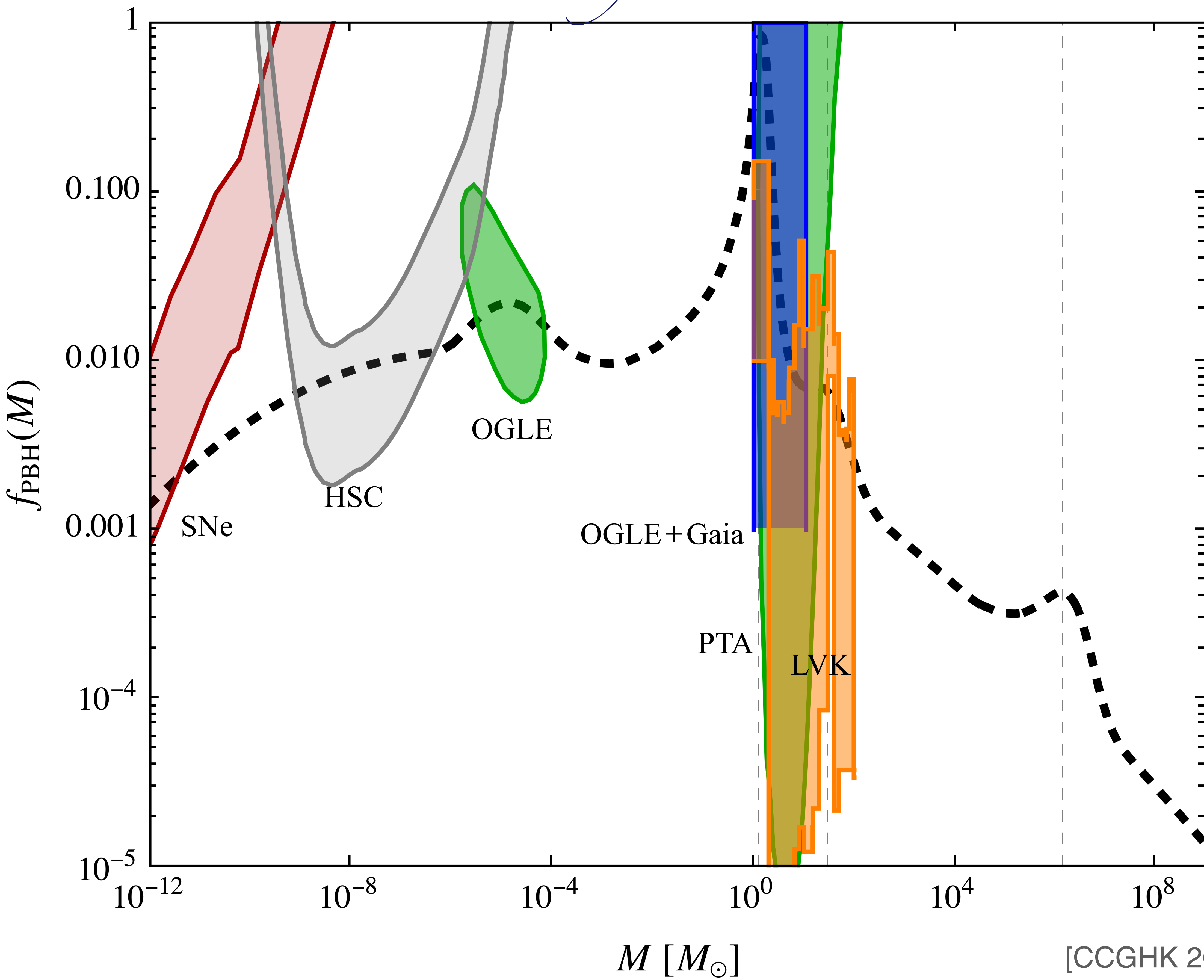

[CCGHK 2023]

PBH Mass Function — Confronted with Observations

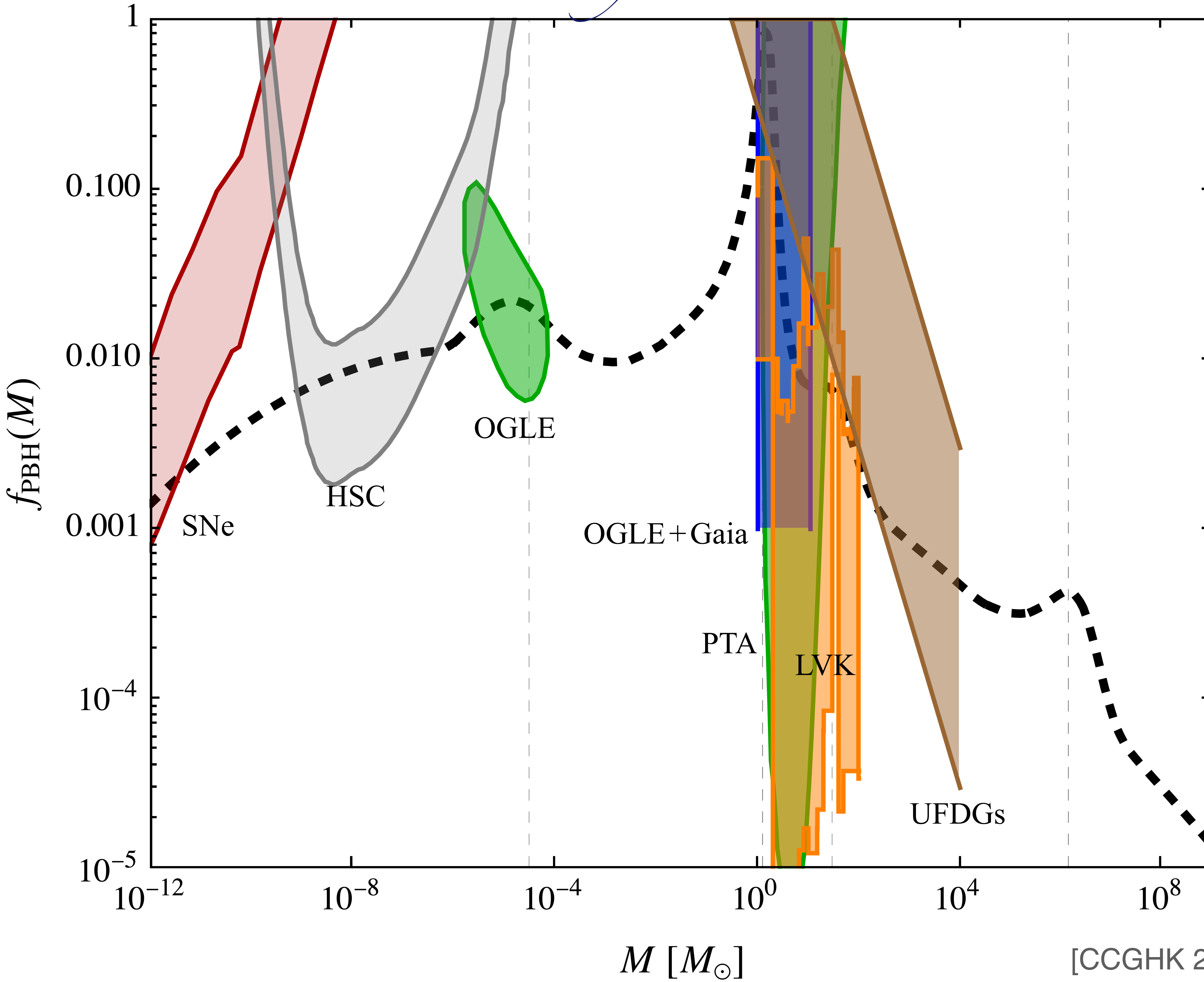

[CCGHK 2023]

PBH Mass Function — Confronted with Observations

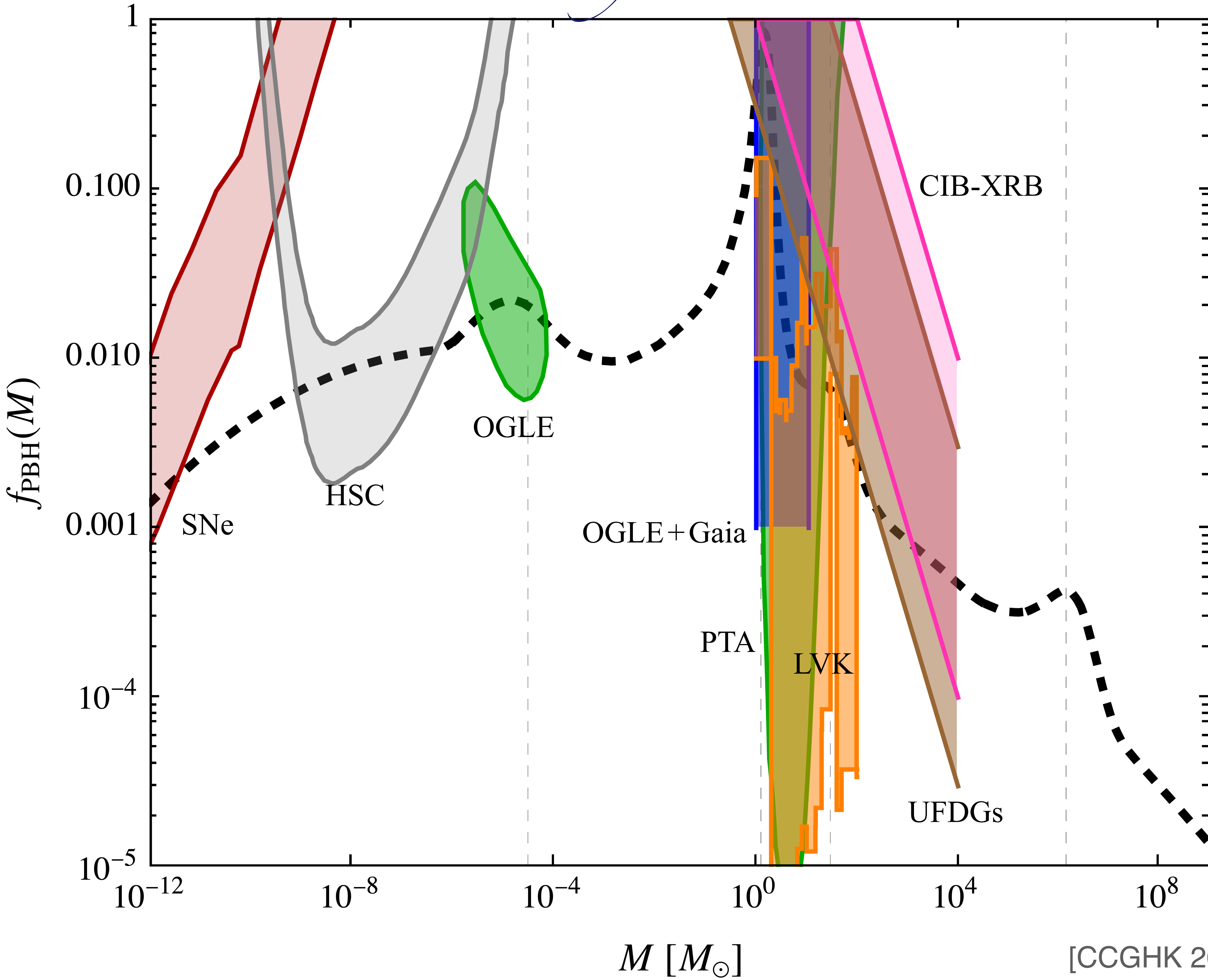

[CCGHK 2023]

PBH Mass Function — Confronted with Observations

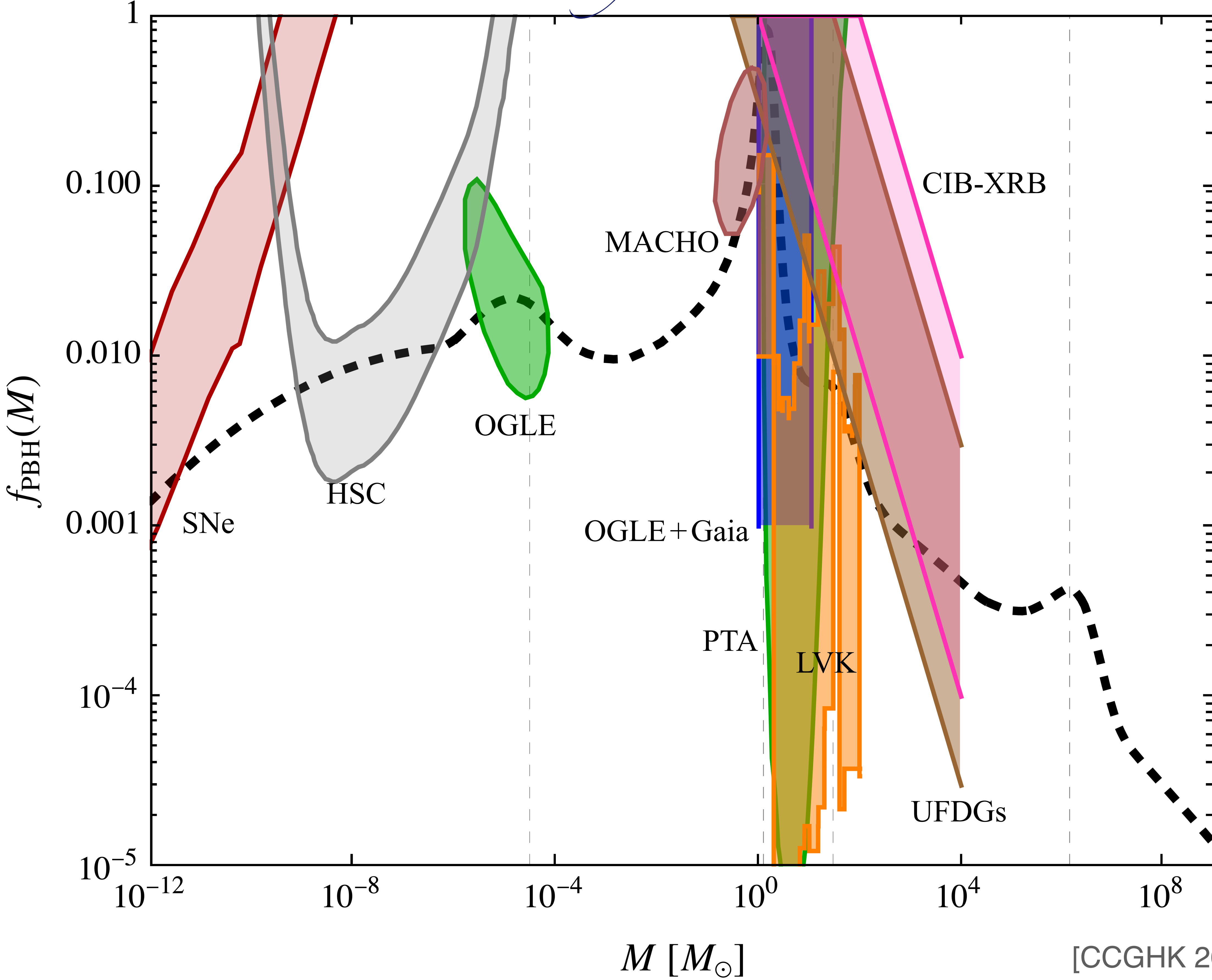

[CCGHK 2023]

PBH Mass Function — Confronted with Observations

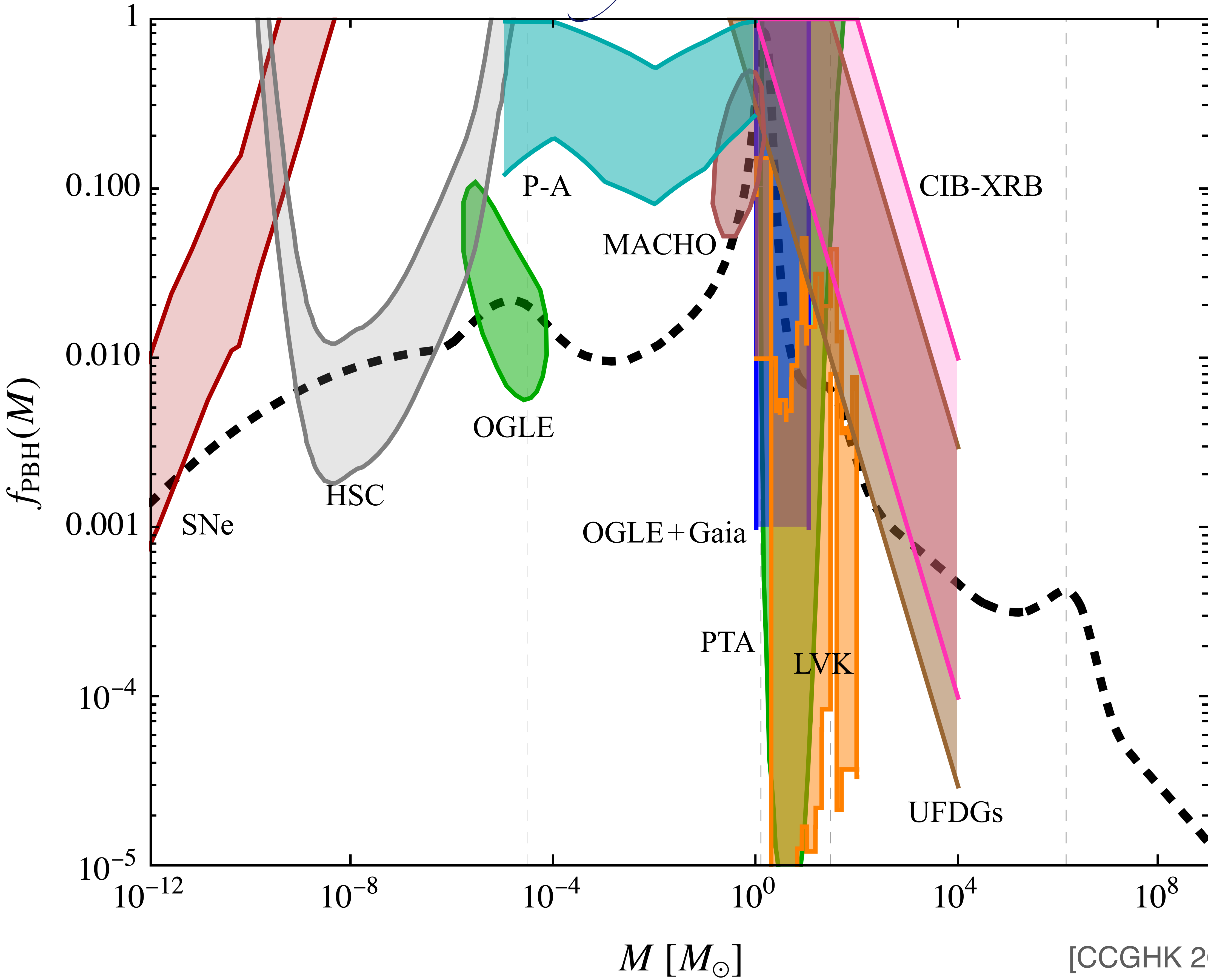

[CCGHK 2023]

PBH Mass Function — Confronted with Observations

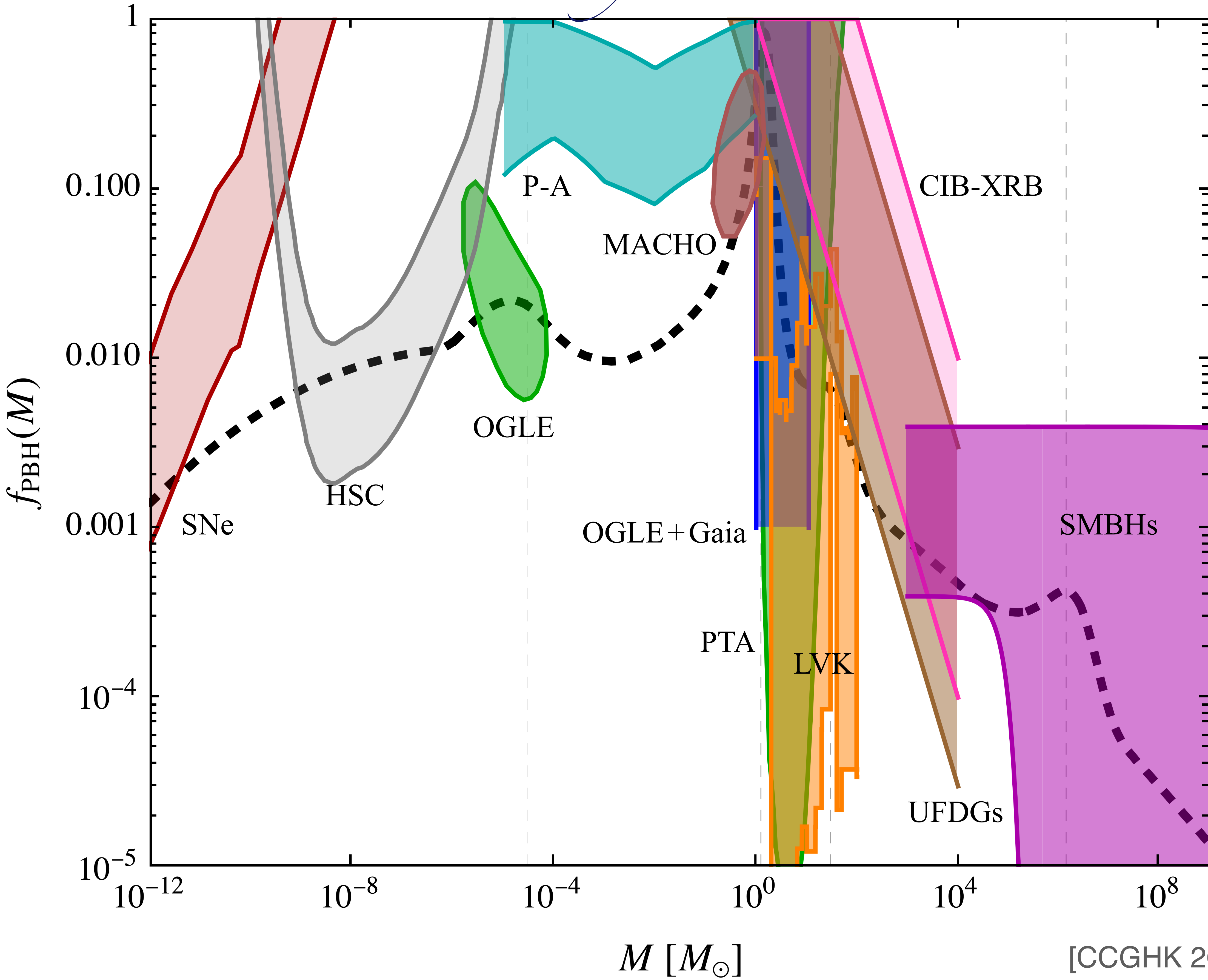

[CCGHK 2023]

Connecting all Positive Evidences!

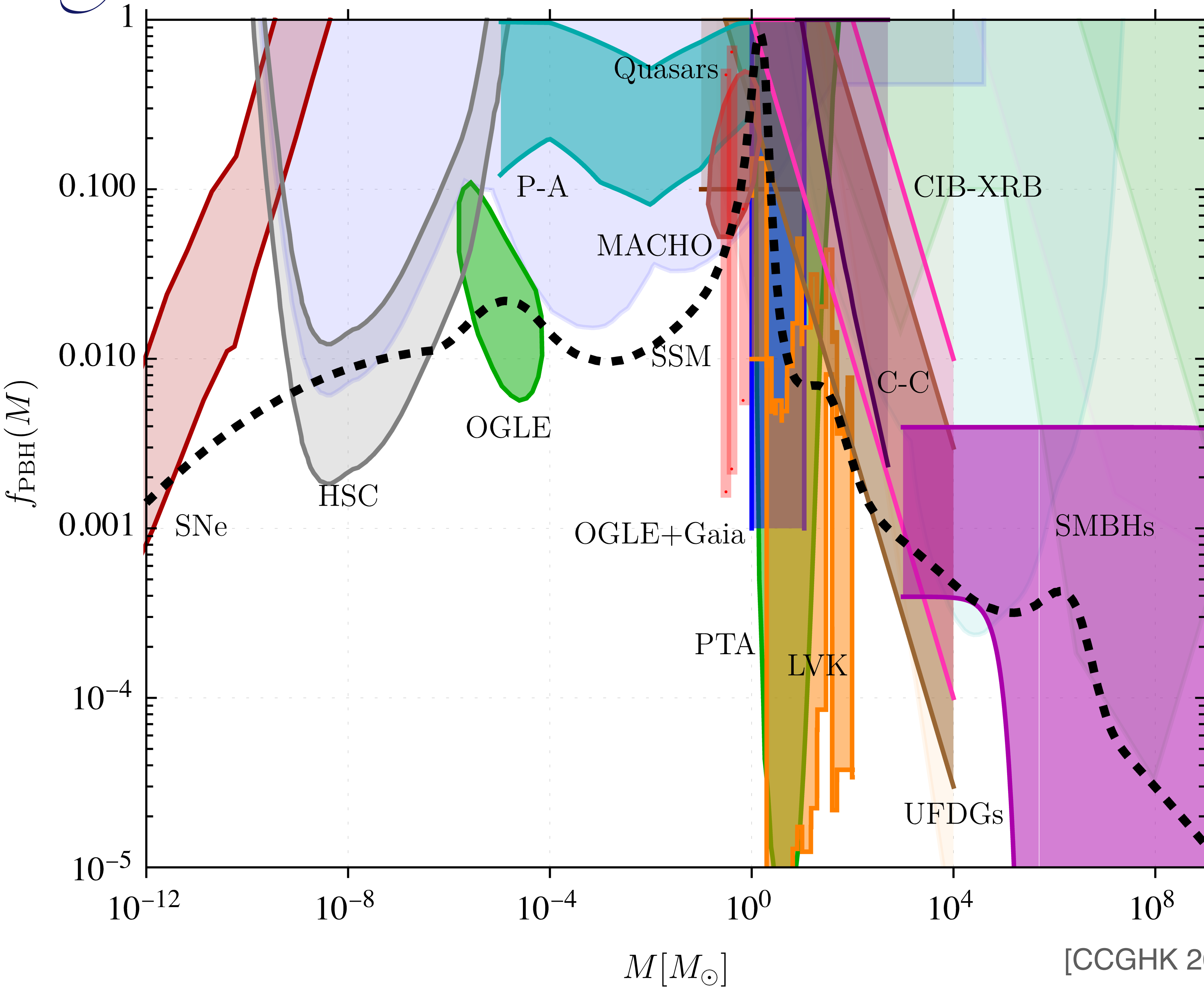

[CCGHK 2023]

Shall Ye Become Positivists!

Observational Evidence for Primordial Black Holes: A Positivist Perspective

B. J. Carr,[1,*] S. Clesse,[2,†] J. García-Bellido,[3,‡] M. R. S. Hawkins,[4,§] and F. Kühnel[5,¶]

[1] *School of Physics and Astronomy, Queen Mary University of London*

[2] *Service de Physique Théorique, University of Brussels (ULB)*

[3] *Instituto de Física Teórica, Universidad Autonóma de Madrid*

[4] *Royal Observatory Edinburgh*

[5] *Max Planck Institute for Physics,*

(Dated: Wednesday 7th June, 2023, 12:34am)

We review numerous arguments for primordial black holes (PBHs) based on observational evidence from a variety of lensing, dynamical, accretion and gravitational-wave effects. This represents a shift from the usual emphasis on PBH constraints and provides what we term a positivist perspective. Microlensing observations of stars and quasars suggest that PBHs of around $1\,M_\odot$ could provide much of the dark matter in galactic halos, this being allowed by the Large Magellanic Cloud observations if the PBHs have an extended mass function. More generally, providing the mass and dark matter fraction of the PBHs is large enough, the associated Poisson fluctuations could generate the first bound objects at a much earlier epoch than in the standard cosmological scenario. This simultaneously explains the recent detection of high-redshift dwarf galaxies, puzzling correlations of the source-subtracted infrared and X-ray cosmic backgrounds, the size and the mass-to-light ratios of ultra-faint-dwarf galaxies, the dynamical heating of the Galactic disk, and the binary coalescences observed by LIGO/Virgo/KAGRA in a mass range not usually associated with stellar remnants. Even if PBHs provide only a small fraction of the dark matter, they could explain various other observational conundra, and sufficiently large ones could seed the supermassive black holes in galactic nuclei or even early galaxies themselves. We argue that PBHs would naturally have formed around the electroweak, quantum chromodynamics and electron-positron annihilation epochs, when the sound-speed inevitably dips. This leads to an extended PBH mass function with a number of distinct bumps, the most prominent one being at around $1\,M_\odot$, and this would allow PBHs to explain much of the evidence in a unified way.

Addendum

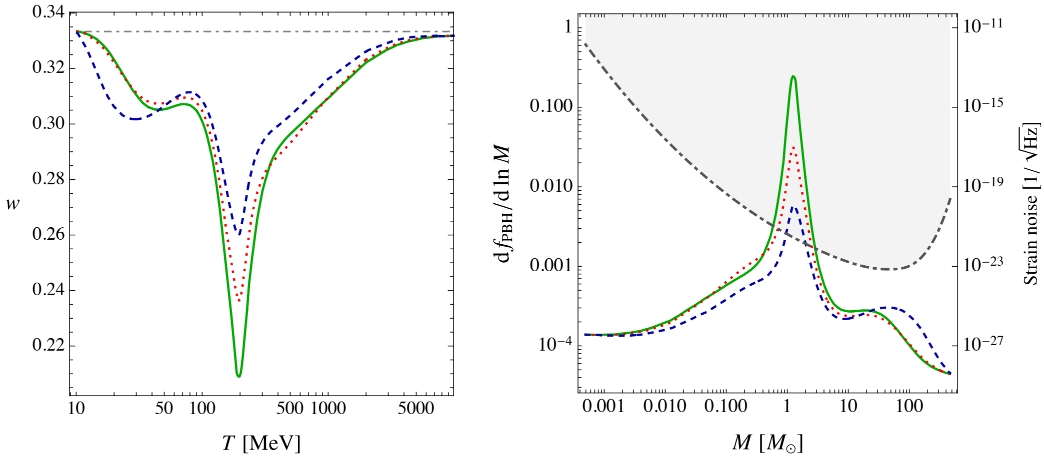

Figure 37. *Left panel:* Effective equation-of-state parameter as a function of temperature. Shown are the three cases of different lepton flavour asymmetry and the 1/3 for a radiation fluid. The standard scenario [case (1)] is indicated by the green solid line. *Right panel:* Spectral density of the PBH dark matter fraction as a function of PBH mass, for the three cases. The green solid line indicates the standard scenario. Also shown is the LIGO sensitivity curve (grey dot-dashed line) from Ref. [242], for equal-mass mergers and using the maximal GW frequency $f_{\max} \approx 4400\, M_\odot/M$ for the conversion from frequency to mass.

The left panel of Fig. 37 shows how non-zero flavour asymmetries weaken the softening of w during the transition, with even $\ell_e = 0$ yielding a pronounced effect. Two cases of unequal lepton flavour asymmetry are chosen for illustrative purposes. Note that a lepton flavour asymmetry always weakens the softening of the equation of state during the QCD transition, as it adds leptons to the Universe which do not interact strongly. This is different from the smaller effect at the pion/muon plateau, where lepton flavour asymmetries can lead to either stiffening or softening (cf. the two cases of unequal flavour asymmetry) as pions and muons become non-relativistic. The corresponding result for the PBH dark matter fraction is depicted in the right panel of Fig. 37. Due to the exponential enhancement of Eq. (VII.7), the three cases differ significantly. The effect of lepton flavour asymmetries are currently being explored. As shown by Gao & Oldengott [401], the cosmic QCD transition might even become first order if the asymmetries are sufficiently large, with a dramatic impact on the PBH mass function.

D. Comparing Evidence with Thermal-History Model

In Figs. 1 and 38, we have indicated the PBH mass and dark matter fraction required to explain the various type of observational evidence discussed in this review. We now explain the derivation of these regions in more detail, considering the lensing, dynamical and GW arguments in turn. However, just as for PBH constraints, all these estimates are based on various assumptions and subject to significant uncertainties. In particular PBH properties (such as mass function, clustering etc.) can modify the different regions. Unless indicated otherwise, we assume a monochromatic PBH mass function.

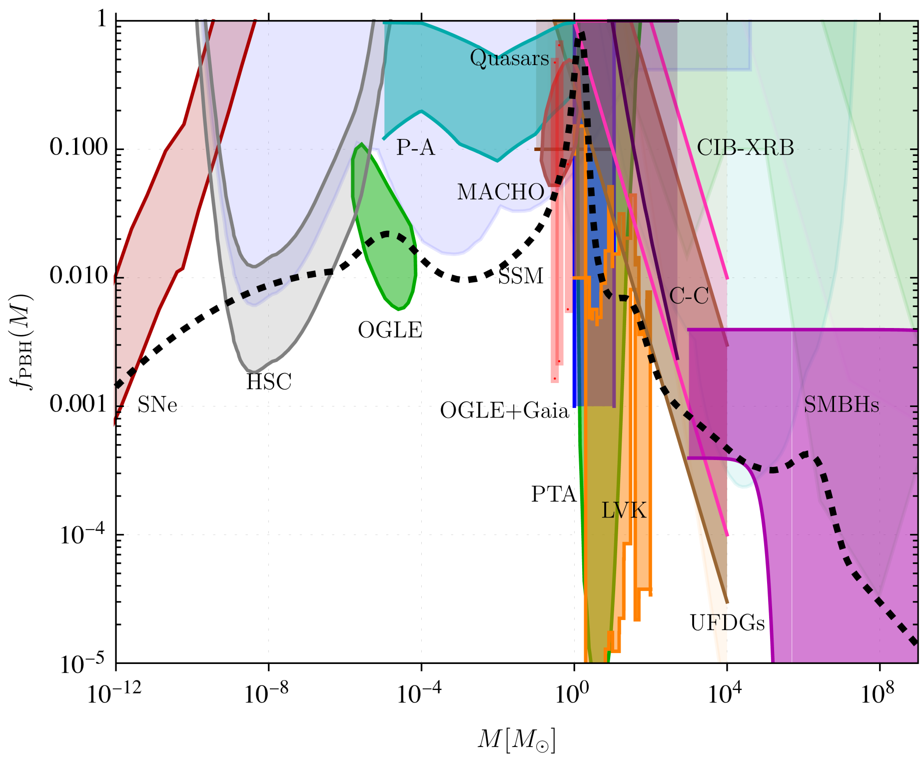

Figure 38. PBH mass function with peaks induced by the thermal history of the Universe (thick, dashed curve; cf. Ref. [34]). Figure includes the same pieces of positive evidence for PBHs as in Fig. 1. Also included, as a comparison, are various monochromatic constraints on $f_{\rm PBH}(M)$ (light-shaded regions), taken from Ref. [402].

PBH dark matter fraction from lensing evidence. We have estimated the PBH dark matter fraction for six types of lensing evidence in the following way:

- *For HSC*, we have reinterpreted the limits of Ref. [98]. Instead of assuming no detection, we have computed the 2σ confidence intervals for $f_{\rm PBH}$ assuming that one PBH microlensing event was observed. The limit is identified with a band using simple Poisson statistics. All the assumptions are therefore identical to those of Ref. [98].
- *For OGLE*, we show the 2σ allowed region provided in Fig. 8 of Ref. [95], combining the OGLE confidence region with the HSC exclusion region
- *For POINT-AGAPE pixel-lensing (P-A)*, we provide a band of possible $f_{\rm PBH}$ values based on the Table 9 of Ref. [97], where 2σ confidence intervals were estimated for different PBH masses.
- *For quasars*, there is not yet a robust estimation of a confidence region despite the fact that we consider them as a strong evidence for a large fraction of dark matter made of compact objects. We therefore consider a relatively broad range of PBH masses, between $10^{-2}\,M_\odot$ and $10\,M_\odot$, and a lower limit of $f_{\rm PBH} > 0.1$, but these are only order-of-magnitude estimates.
- *For MACHO*, the 2σ region comes from Refs. [69, 403]. We have argued that the MACHO microlensing events are real and plausibly due to PBHs, despite EROS and OGLE later claiming more stringent limits.

- *For OGLE+Gaia*, we assume that all the microlensing events are due to PBHs. The indicated band comes from the lowest and highest mean masses shown in Fig. 7, obtained by the analysis of Ref. [92], and there is a somewhat arbitrary lower bound, $f_{\rm PBH} \approx 10^{-3}$, below which PBHs are unlikely to explain so many microlensing events.

All these estimates are subject to large uncertainties. In particular, the size of PBH clusters could alter the PBH fraction inferred from microlensing of stars towards the Magellanic Clouds. Figure 1 represents the ideal situation, in which all the observations are due to PBHs. However, since alternative origins are not excluded, it is possible that only a some of them are.

PBH dark matter fraction from dynamical and accretion evidence. We have estimated the PBH dark matter fraction for the five types of dynamical and accretion evidence as follows:

- *For SNe*, the band corresponds to the one shown in Fig. 20, which is taken from Ref. [186].
- *For UFDGs*, we assume $0.3 < f_{\rm PBH}\, m_{\rm PBH}/M_\odot < 30$, with a maximum mass of $10^4\, M_\odot$. These values are somewhat arbitrary and do not result from a robust statistical analysis, but the large cosmological, astrophysical and observational uncertainties would limit the validity of a more refined analysis. The values shown correspond to the two extreme cases displayed in Fig. 5. With our simple modelling of PBH clustering, these values could simultaneously explain (1) the minimum size of observed UFDGs, (2) the relation between their radius and mass, and (3) their very large mass-to-light ratios due to PBH gas accretion.
- *For C-C (core-cusp)*, the displayed region is based on the lower limits from Fig. 7 of Ref. [167], extrapolated up to a mass of $10^3\, M_\odot$ since there is no theoretical restriction on this, other than there being enough PBHs for dynamical heating to be efficient.
- *For CIB-XRB correlations*, the band corresponds to $1 < f_{\rm PBH}\, m_{\rm PBH}/M_\odot < 100$ up to a mass of $10^4\, M_\odot$. We have not used a rigorous statistical analysis to get more precise values but the proposed band agrees with the order-of-magnitude estimate in Ref. [48].
- *For SMBHs*, we have followed Ref. [34] in assuming a linear relation between the central IMBH or SMBH, as suggested by the gray band in Fig. 1 of Ref. [404], as well as a Press–Schechter halo mass function. The upper limit neglects the effects of accretion and mergers. The origin of IMBHs and SMBHs in clusters and galaxies is therefore related to the PBH mass distribution. The lower limit assumes that the PBH mass increased during the pregalactic era at the Bondi rate, given by Eq. (IV.6), until it reached the Eddington limit, given by Eq. (IV.9). However, this is subject to the large uncertainties in the accretion process. We note that Fig. 36 suggests $f(M) \propto M^{-1/4}$ for $M > 10\, M_\odot$ in the thermal-history model, which corresponds to a power-law function with $\alpha \approx 9/4$.

The proposed regions depend on the very uncertain physical processes which underlie the dynamical evolution of PBH clusters and the accretion process throughout cosmic history. Most of the dynamical and accretion evidence relates to the mass range from one to a billion solar masses and therefore complements the microlensing and GW evidence. This clearly favours models with an extended PBH mass distribution. In this case, all the evidence depends on Poisson-induced clustering. Since this is determined by the product $f_{\rm PBH}\, m_{\rm PBH}$, PBHs with different masses would contribute to the effect in such a way that a distribution not crossing the proposed region can still provide the required effect.

Although such extended mass distributions may conflict with the stringent constraints on the CMB distortions and anisotropies, these can be relaxed for realistic accretion models if PBH formation is associated with curvature fluctuations with non-Gaussian tails [405].

PBH dark matter fraction from gravitational-wave evidence. We have estimated that the PBH dark matter fraction for various types of GW evidence. For this purpose, we have considered the merger rates of early binaries for a monochromatic model, but obviously the range of component masses associated with the observed coalescences points to an extended mass distribution.

- *For subsolar-mass candidates*, we have used the three subsolar-mass triggers in the LVK O3b observing run to derive credible 2σ intervals for $f_{\rm PBH}$ in the monochromatic case. More precisely, we use the chirp mass associated with each candidate to compute an associated interval for $f_{\rm PBH}$, this mass being well reconstructed for GW events. In each case, it is sufficiently below $1\,M_\odot$ to guarantee that at least one of the components is a subsolar-mass compact object for a real GW signal. We then assume that the two components have the same mass and use the volume-time sensitivity $\langle VT \rangle$ obtained in Ref. [263] for each mass. When combined with the expected merger rate of early binaries, using simple Poisson statistics, one can compute a 2σ interval for $f_{\rm PBH}$ for each subsolar-mass trigger.
- *For LVK*, we have used the inferred merger rates in intervals at different masses, for the O1, O2 and O3 runs and the binned Gaussian process model of Ref. [239], considering only the rates for equal-mass mergers shown in their Fig. 4 (orange regions). For each bin, we have then compared this with the expected merger rates of early binaries for a monochromatic model to infer the 90% CL intervals for $f_{\rm PBH}$. This model does not allow $f_{\rm PBH}$ to reach 1 but it could still exceed 0.1 at solar-mass scale, bearing in mind the uncertainties associated with the rate model.
- *For PTAs*, we have used the two-dimensional marginalised posterior distributions of the primordial power spectrum amplitude and pivot wavelength mode calculated for IPTA observations in Ref. [284], as shown in Fig. 30; this assumes a log-normal primordial power spectrum. In order to translate these contours into $f_{\rm PBH}$ constraints, we have assumed a critical overdensity threshold for PBH formation at the QCD epoch and a corresponding PBH abundance in agreement with the recent numerical simulations of Ref. [228]. The obtained region is extremely sensitive to the threshold values and the method used to compute the PBH abundance, so it can vary by several orders of magnitudes.

The uncertainties and model dependence of the merger rates, the exact PBH formation mechanism, and the various possibilities for the statistics of the curvature fluctuations, clearly blur the calculated intervals for GW mergers and PTAs. Nevertheless, GW observations hint at a peak in $f_{\rm PBH}$ at the solar-mass scale, as expected for PBHs forming at QCD epoch. These observations complement and agree well with the lensing, dynamical and accretion evidence. The fit with the data is consistent with all the constraints if one uses a running spectral index for the power spectrum at PBH scales, as suggested in Ref. [406]. In this case, we are considering a spectral tilt $n_{\rm s} = 0.986$ and running $\alpha_{\rm s} = -0.0018$ at PBH scales. These values are remarkably close to those measured at CMB scales, which may hint that Critical Higgs Inflation generates the full matter power spectrum.